Title: Obesity promotes breast epithelium DNA damage in *BRCA* mutation carriers

Authors: Priya Bhardwaj[1], Neil M. Iyengar[1,2], Heba Zahid[3], Katharine M. Carter[1], Dong Jun Byun[4], Man Ho Choi[4], Qi Sun[5], Oleksandr Savenkov[6], Charalambia Louka[1], Catherine Liu[1], Phoebe Piloco[1], Monica Acosta[1], Rohan Bareja[7], Olivier Elemento[7], Miguel Foronda[8], Lukas E. Dow[1,9], Sofya Oshchepkova[1], Dilip D. Giri[10], Michael Pollak[11], Xi Kathy Zhou[6], Benjamin D. Hopkins[12], Ashley M. Laughney[9], Melissa K. Frey[13], Lora Hedrick Ellenson[10], Monica Morrow[14], Jason A. Spector[15], Lewis C. Cantley[9], Kristy A. Brown[1,9*]

Affiliations:

[1]Department of Medicine, Weill Cornell Medicine; New York, USA.

[2]Department of Medicine, Memorial Sloan Kettering Cancer Center; New York, USA.

[3]Department of Medical Laboratory Technology, College of Applied Medical Science, Taibah University; Medina, Saudi Arabia.

[4]Center for Advanced Biomolecular Recognition, Korea Institute of Science and Technology, Seoul, Korea.

[5]Computational Biology Service Unit of Life Sciences Core Laboratories Center, Cornell University, Ithaca; USA.

[6]Department of Population Health Sciences, Weill Cornell Medicine; New York, USA.

[7]Caryl and Israel Englander Institute for Precision Medicine, Weill Cornell Medicine; New York, USA.

[8]Department of Neurology, Memorial Sloan Kettering Cancer Center; New York, USA.

[9]Sandra and Edward Meyer Cancer Center, Weill Cornell Medicine; New York, USA.

[10]Department of Pathology, Memorial Sloan Kettering Cancer Center; New York, USA.

[11]Departments of Medicine and Oncology, McGill University; Montreal, Canada.

[12]Department of Genetics and Genomic Sciences, Icahn School of Medicine at Mount Sinai; New York, USA

[13]Department of Obstetrics & Gynecology, Weill Cornell Medicine; New York, USA

[14]Department of Surgery, Memorial Sloan Kettering Cancer Center; New York, USA.

[15]Laboratory of Bioregenerative Medicine & Surgery, Weill Cornell Medicine; New York, USA.

*Corresponding author. Email: kab2060@med.cornell.edu

One Sentence Summary: Elevated body mass index is positively associated with DNA damage in breast epithelium of *BRCA* mutation carriers

Abstract:

Obesity, defined as a body mass index (BMI) ≥ 30, is an established risk factor for breast cancer among women in the general population after menopause. Whether elevated BMI is a risk factor for women with a germline mutation in *BRCA1* or *BRCA2* is less clear due to inconsistent findings from epidemiological studies and lack of mechanistic studies in this population. Here, we show that DNA damage in normal breast epithelium of *BRCA* mutation carriers is positively correlated with BMI and with biomarkers of metabolic dysfunction. Additionally, RNA-sequencing reveals significant obesity-associated alterations to the breast adipose

microenvironment of *BRCA* mutation carriers, including activation of estrogen biosynthesis, which impacts neighboring breast epithelial cells. We found that blockade of estrogen biosynthesis or estrogen receptor activity decreases DNA damage. Additional obesity-associated factors, including leptin and insulin, increase DNA damage in *BRCA* heterozygous epithelial cells, and inhibiting the signaling of these factors with a leptin neutralizing antibody or PI3K inhibitor, respectively, decreases DNA damage. Furthermore, we show that increased adiposity is associated with mammary gland DNA damage and increased penetrance of mammary tumors in *Brca1*+/- mice. Overall, our results provide mechanistic evidence in support of a link between elevated BMI and breast cancer development in *BRCA* mutation carriers, and suggests that maintaining a healthy bodyweight or pharmacologically targeting estrogen or metabolic dysfunction may reduce the risk of breast cancer in this population.

INTRODUCTION

Inheriting a pathogenic mutation in the DNA repair genes *BRCA1* or *BRCA2* is causally linked to the development of breast and ovarian cancer in women (*1, 2*). Although there is strong evidence linking obesity to the development of hormone receptor-positive breast cancer after menopause in the general population (*3*), there are conflicting results in *BRCA* mutation carriers. Some studies have found that maintaining a healthy bodyweight or weight loss in young adulthood is associated with delayed onset of breast cancer (*4, 5*). Other studies have reported that adiposity or elevated bodyweight in adulthood is associated with increased cancer risk (*5-9*). Conversely, some reports indicate that increased body mass index (BMI) in young adulthood may have protective effects, and that risk is modified by menopausal status (*9-11*). The lack of clarity on the role of BMI and risk of breast cancer development in *BRCA* mutation carriers

limits the ability of clinicians to provide evidence-based guidance on prevention strategies beyond prophylactic surgical intervention.

Weight gain and obesity, defined as having a BMI ≥ 30, are often coupled with metabolic syndrome, insulin resistance, and significant changes to adipose tissue, including that of the breast microenvironment (*12-15*). Obesity-induced changes to breast adipose tissue includes dysregulation of hormone and adipokine balance, and increased production of inflammatory mediators (*16*). For example, estrogen biosynthesis is increased in obese breast adipose tissue due to overexpression of aromatase in adipose stromal cells which catalyzes the conversion of androgens to estrogens (*17-19*). Additionally, excessive expansion of adipocytes leads to hypoxia, lipolysis, and altered adipokine production including a higher leptin to adiponectin ratio (*15, 20, 21*). These changes to the breast microenvironment may have important implications for breast carcinogenesis given that breast epithelial cells are embedded in this milieu and engage in epithelium-adipose crosstalk (*22*).

BRCA1 and BRCA2 are critical for their role in homologous recombination-mediated repair of DNA double strand breaks (*23*). Mutations in either *BRCA1* or *BRCA2* cause a defect in DNA repair which can lead to an accumulation of DNA damage and consequently, tumorigenesis (*24, 25*). Studies have linked obesity or metabolic syndrome to DNA damage, including in leukocytes (*26*), skeletal muscle (*27*), peripheral blood mononuclear cells (*28*), and in pancreatic β-cells (*29*), but no studies have examined the relationship between obesity and DNA damage in normal breast epithelial cells.

We show that BMI and markers of metabolic dysfunction are positively correlated with DNA damage in normal breast epithelium of women carrying a *BRCA* mutation, a finding that is extended to the fallopian tube of *BRCA* mutation carriers. RNA-sequencing of whole breast

tissue and of isolated breast epithelial organoids from *BRCA* mutation carriers, along with *ex vivo* and *in vitro* studies with *BRCA1* and *BRCA2* mutant primary tissues and cell lines, suggests several obesity-associated factors as possible drivers of DNA damage. Additionally, metformin, fulvestrant, leptin neutralizing antibodies and a PI3K inhibitor reduce damage induced by the breast microenvironment of women with obesity. *In vivo* studies in *Brca1* heterozygous knockout mice demonstrate that high-fat diet-induced obesity leads to glucose intolerance in association with elevation in epithelial cell DNA damage and greater mammary tumor penetrance relative to mice fed a low-fat diet. The data presented provide mechanistic evidence supporting an increased risk of breast cancer development in *BRCA* mutation carriers with elevated BMI and metabolic dysfunction, and importantly, provides clinically-relevant strategies for risk reduction.

RESULTS

Elevated BMI positively correlates with breast epithelial cell DNA damage in women carrying a mutation in *BRCA1* or *BRCA2*

To assess levels of DNA damage in normal breast epithelium in association with BMI in women carrying a *BRCA1* or *BRCA2* mutation, tissue microarrays were constructed from non-cancerous breast tissue obtained from 69 women undergoing mastectomy. The study population included *BRCA1* (n=40) and *BRCA2* (n=29) mutation carriers who had documented body mass index (BMI, kg/m^2) between 19.38 and 44.9 (median 23.9) at the time of surgery as shown in **Table 1**. When grouping the population by BMI category of healthy weight (BMI $\leq$ 24.9 kg/m^2, n=43) or overweight/obese (BMI $\geq$ 25.0 kg/m^2, n=26), median age is significantly higher in the group with overweight/obesity compared to the group with healthy weight (44.5 vs 39.0,

115 respectively, *P*=0.03). Additional clinical features elevated in the group with overweight/obesity
116 compared to the group with healthy weight include percent of subjects diagnosed with
117 dyslipidemia (23.1% vs 2.3%, *P*=0.01) and with hypertension (23.1% vs 4.7%, *P*=0.046). The
118 group with healthy weight also has a greater representation of pre-menopausal vs post-
119 menopausal subjects compared to the group with overweight/obesity (*P*=0.022). Diagnosis of
120 diabetes, race, presence of invasive tumor, tumor subtype and *BRCA1* vs *BRCA2* mutation were
121 not significantly different between the two BMI groups (**Table 1**).

122 Immunofluorescence staining for the DNA double-strand break marker γH2AX was
123 performed with nuclear counterstain Hoechst to visualize the number of foci of DNA damage per
124 epithelial cell (**Fig. 1A**). Among *BRCA1* and *BRCA2* mutation carriers, but not among women
125 with no identified mutation in *BRCA*, BMI was positively associated with breast epithelial cell
126 DNA damage as quantified by # of γH2AX foci/100 cells (**Fig. 1B & 1C**). Age was also found to
127 be significantly correlated with DNA damage (**Fig. 1D**). While this correlation diminished when
128 adjusting for BMI (*P*=0.335, **Table 2**), BMI remained positively associated with DNA damage
129 when adjusting for age (*P*=0.003, **Table 2**). Post-menopausal women were found to exhibit
130 modestly higher levels of DNA damage compared to pre-menopausal women (**Fig. 1E**).
131 However, this difference was not significant. Additionally, circulating levels of sex hormone
132 binding globulin (SHBG), which binds estrogens to decrease their bioavailability, were
133 negatively correlated with breast epithelial cell DNA damage (**Fig. 1F**). This negative
134 association remains significant when adjusting for age, but not BMI (*P*=0.020 and *P*=0.081,
135 respectively, **Table 2**). Elevated BMI is often coupled to insulin resistance, a hallmark of
136 metabolic dysfunction. Accordingly, fasting serum levels of insulin and HOMA2 IR were
137 positively correlated with levels of breast epithelial cell DNA damage while glucose was not

(Fig. 1G-I). Insulin and HOMA2 IR retained significance after adjustments for either BMI (P=0.009 and P=0.010, respectively) or age (P<0.001 for both, **Table 2**). No correlation with DNA damage was observed for circulating biomarkers of inflammation including high-sensitivity C-reactive protein (hsCRP) and interleukin-6 (IL-6) or with crown-like structures (CLS), a histological marker of local breast adipose inflammation (*30*) (**Fig 1. J-L**). These data indicate that among *BRCA* mutation carriers, elevated BMI is a risk factor for breast epithelial cell DNA damage. Furthermore, specific obesity-associated factors including insulin resistance and estrogen balance may be important drivers of this risk.

Elevated BMI is associated with significant differences in gene expression in breast adipose tissue and in breast epithelial cells of *BRCA* mutation carriers

To identify changes associated with obesity in breast epithelial cells and in the breast adipose microenvironment that may be linked to DNA damage, we conducted RNA-seq studies on both isolated primary breast epithelial cells and non-cancerous whole breast tissue obtained from *BRCA1* and *BRCA2* mutation carriers.

RNA-seq was conducted on breast tissue pieces obtained from *BRCA* mutation carriers with BMI < 25 kg/m^2 (n=64) and with BMI ≥ 25 kg/m^2 (n=67). An unsupervised heatmap was constructed which shows general clustering of cases with BMI < 25 and clustering of cases with BMI ≥ 25 by gene expression (**Fig. 2A**). 2329 genes were significantly upregulated with obesity and 1866 were significantly downregulated (**Table S1**). Ingenuity Pathway Analysis (IPA) identified several pathways that were significantly altered in the cases with BMI ≥ 25 which include pathways associated with obesity and metabolic dysfunction, such as “Phagosome

Formation", "LXR/RXR Activation", "Tumor Microenvironment Pathway Activation", and "Estrogen Biosynthesis" (**Fig. 2B**). A heatmap of genes involved in estrogen regulation shows a significant increase in many genes involved in the bioactivity, biosynthesis and activation of estrogens, including steroid sulfatase, 3βHSD1, AKR1C3, AKR1B15, 17βHSD1 and aromatase (CYP19A1) (**Fig. 2C**). Conversely, gene expression of 17βHSD8, involved in estrogen inactivation, was significantly lower in cases with BMI ≥ 25 relative to cases with BMI < 25. Moreover, there were mixed effects of obesity on the expression of genes involved in estrogen catabolism to hydroxylated metabolites and neutralization by COMT.

To explore which changes in the breast microenvironment are associated with DNA damage in breast epithelial cells, we analyzed breast tissue pathway changes in relation to level of epithelial cell DNA damage quantified by γH2AX immunofluorescence staining (**Fig. 2D**; n=61). The level of epithelial cell DNA damage in each case was stratified by quartiles and breast tissue gene expression was compared in the highest quartile (Q4) relative to the lowest quartile (Q1), independent of BMI (**Table S2**). The top 15 canonical pathways activated in Q4 vs Q1 breast tissue are shown (**Fig. 2D**) with several pathways being common to both DNA damage and BMI analyses (**Fig. 2D** vs **Fig. 2B**). Although the estrogen biosynthesis pathway was found to be activated in tissue from cases with BMI ≥ 25 compared to cases with BMI < 25 (**Fig. 2B**, z-score=0.775, *P* value=1.14×10^{-6}), a stronger activation score is found when comparing DNA damage Q4 vs Q1 (**Fig. 2D**, z-score=2.646, *P* value=2.7×10^{-3}), suggesting that tissue estrogen biosynthesis is highly correlated with level of breast epithelial cell DNA damage, irrespective of BMI.

Breast epithelial organoids were isolated from *BRCA* mutation carriers with BMI < 25 (n=10) or with BMI ≥ 25 (n=9) at the time of surgery. To validate and characterize the isolated

epithelial organoids, immunofluorescence staining was conducted for cytokeratin 8 (CK8) and cytokeratin 14 (CK14), characteristic markers of luminal and basal epithelial cells, respectively, that are known to comprise the breast epithelium (**Fig. 2E**). 1144 genes were significantly upregulated and 537 genes were significantly downregulated in organoids from women with BMI ≥ 25 relative to organoids from women with BMI < 25 (**Table S3**). The top 20 canonical pathways identified by IPA as regulated in the organoids from women with BMI ≥ 25 are shown (**Fig. 2F**) and include activation of pathways known to be associated with obesity, including "HIF1α signaling", "IL-8 signaling", "ERK/MAPK signaling", and "PI3K/AKT signaling", among others.

To start deciphering mechanisms that would account for differences in the impact of BMI on DNA damage in *BRCA* mutation carriers versus non-carriers (**Fig. 1B and 1C**), we also conducted RNA-seq on organoids isolated from age-matched women WT for *BRCA* with BMI < 25 (n=11) or with BMI ≥ 25 (n=8). 750 genes were significantly upregulated and 659 genes were significantly downregulated in organoids from non-carriers with BMI ≥ 25 relative to organoids from women with BMI < 25 (**Table S4**). The top 20 canonical pathways regulated in organoids from non-carriers with BMI ≥ 25 showed little overlap with pathways regulated in organoids from *BRCA* mutation carriers (**Fig. S1A vs Fig. 2F**), with a direct comparison of z-scores and pathway activation or deactivation shown in **Fig. S1B**.

Collectively, these RNA-seq studies show that *BRCA1* and *BRCA2* mutation carriers who have overweight/obesity as defined by BMI ≥ 25 have significantly altered breast epithelial cell and breast adipose microenvironment gene expression compared with carriers with BMI < 25, and provide a rationale for further exploring whether estrogens are a driver of DNA damage in breast epithelial cells from *BRCA* mutation carriers. While elevated BMI was also associated

with significant gene expression changes to breast epithelial cells from non-carriers, the changes observed in relation to BMI were distinct from those found in *BRCA* mutation carriers which may help to explain differences in correlation data between BMI and DNA damage among these two populations.

Crosstalk between epithelial cells and the breast adipose microenvironment

Given the significant gene expression changes identified in *BRCA* heterozygous breast adipose tissue and in breast epithelial cells in association with elevated BMI, we next investigated whether the breast adipose microenvironment drives gene expression in breast epithelial cells. IPA Upstream Regulator tool was used to identify regulators of gene expression differences in organoids isolated from *BRCA* mutation carriers with overweight/obesity relative to organoids isolated from carriers with healthy weight. To highlight endogenous factors that may be responsible for driving gene expression changes, results were filtered to show the top 20 secreted factors. Among these factors, beta-estradiol (an estrogen) is the top predicted upstream regulator (**Table 3**). A number of additional predicated upstream organoid regulators are significantly upregulated in breast tissue from *BRCA* mutation carriers with overweight/obesity, including several interleukins (IL2, IL15, and IL5), TGFβ1, CSF1, ANGPT2, and WNT5A. Some factors, such as insulin, are known to be elevated in obesity, but are not produced locally in breast tissue and therefore do not have an observed tissue gene expression level. These data suggest that some endogenously produced factors in the breast microenvironment of women with overweight/obesity may interact with neighboring breast epithelial cells to induce gene expression changes and DNA damage.

Targeting estrogen in breast tissue from *BRCA* mutation carriers reduces epithelial cell DNA damage

Next, we conducted mechanistic studies to determine whether targeting estrogen signaling or biosynthesis in breast tissue would lead to decreased levels of breast epithelial cell DNA damage. We first conducted immunohistochemistry (IHC) staining to verify that normal epithelium from *BRCA1* and *BRCA2* mutation carriers express the estrogen receptor (ERα). Epithelial cells staining positively for ERα were found throughout the epithelium among carriers of *BRCA1* or *BRCA2* mutations (representative images shown in **Fig. 3A, top row**). IF staining was then conducted to visualize whether γH2AX foci co-localize with ERα positive cells. Representative images are shown which highlight ERα positive cells frequently staining positively for γH2AX foci (**Fig. 3A, bottom row**). Next, we tested whether disrupting estrogen signaling through use of the drug fulvestrant, which degrades the estrogen receptor, would impact levels of DNA damage in the breast. Breast tissue was obtained from *BRCA* mutation carriers undergoing surgery (n=7) and were plated as explants in the presence of fulvestrant (100μM) or vehicle for 24 hours (**Fig. 3B**). Explants were formalin fixed and sectioned for assessment of breast epithelial cell DNA damage by IF staining. An approximately 32.5% reduction in DNA damage was observed overall after treatment with fulvestrant (**Fig. 3C**).

Next, we hypothesized that targeting estrogen biosynthesis in the breast by downregulating aromatase expression would lead to less estrogen exposure to the epithelial cells, and consequently decreased DNA damage. In support of this hypothesis, RNA-seq data from *BRCA1* and *BRCA2* mutation carriers showed a positive correlation between breast adipose aromatase expression and level of breast epithelial cell DNA damage (**Fig. 3D**). Importantly, since aromatase expression is known to be upregulated in association with obesity, we conducted

additional statistical analyses to adjust for BMI and found that aromatase remained independently positively associated with DNA damage (P=0.030). To target estrogen biosynthesis, we utilized metformin, a widely used antidiabetic drug which has also been shown to decrease aromatase production in the breast via stimulation of AMP-activated protein kinase (AMPK) in adipose stromal cells (*31, 32*). Breast tissue obtained from *BRCA* mutation carriers (n=3) were plated as explants and treated with metformin (0-100μM) for 24 hours followed by IF assessment of breast epithelial cell DNA damage. A dose-dependent decrease in DNA damage was observed with significant differences after 75 and 100μM of metformin treatment (**Fig. 3E**). Since metformin is known to decrease aromatase expression in adipose stromal cells surrounding breast epithelial cells, we digested breast tissue to isolate the epithelial cells from their microenvironment (**Fig. 3B**) and treated them with metformin for 24 hours to determine if the presence of the breast microenvironment is required for the effect of metformin on DNA damage. Although there was a modest trend for reduction in DNA damage with increasing doses of metformin, these results were not significant (**Fig. 3F**). Consistently, tissue levels of estradiol (E2) were markedly reduced in breast explants after 24-hour metformin treatment in a dose-dependent manner (**Fig. 3G**). Additionally, testosterone and androstenedione, which are converted to E2 and estrone (E1) by aromatase, respectively, were increased in explants following treatment with metformin while both E1 and E2 decreased (**Fig. 3H**). These data show that metformin treatment leads to decreased estrogen biosynthesis in breast tissue in association with reduction in epithelial cell DNA damage.

Local and systemic factors contribute to DNA damage in *BRCA1* and *BRCA2* heterozygous breast epithelial cells

Our data support a paracrine interaction between adipose tissue and breast epithelial cells. Having found a direct role for estradiol in mediating DNA damage in primary human tissues, we next explored the role of additional obesity-associated factors, including those present in breast adipose tissue conditioned media (CM), as well as recombinant leptin and insulin. To first investigate whether factors derived from breast adipose tissue have the ability to directly induce DNA damage in *BRCA* mutant breast epithelial cells, *BRCA1* heterozygous knockout MCF-10A cells were treated with CM from reduction mammoplasty or non-tumor quadrants of mastectomy tissue (**Fig. 4A**, n=36, BMI: 20.6-40.1 kg/m^2). Breast adipose CM treatment was positively correlated with DNA damage as a function of the patient's BMI, as measured by immunofluorescence of γH2AX foci (**Fig. 4B**). Representative confocal images are shown in **Fig. S2**. To determine whether effects of CM on DNA damage were generalizable to *BRCA2* mutation carriers, a subset of CM cases (n=13) were tested in MCF-10A cells carrying a heterozygous *BRCA2* mutation, generated using CRISPR-Cas9 gene editing (see **Supplementary Materials**). A positive correlation between BMI and DNA damage was also observed in these cells (**Fig. 4C**). Representative confocal images are shown in **Fig. S2**. These studies demonstrate that factors secreted by breast adipose tissue directly stimulate DNA damage in breast epithelial cells. Furthermore, given the lack of estrogen receptor expression in MCF-10A cells (*33*), these studies also highlight the existence of additional factors beyond estrogen that may be contributing to DNA damage induction in the setting of obesity in *BRCA1* and *BRCA2* mutant breast epithelial cells.

The expression of leptin, known to be directly correlated with adiposity, is significantly higher in the breast tissue of *BRCA* mutation carriers with a BMI ≥ 25 compared to those with a BMI < 25 (**Table S1**, log2FC= 0.61, P=3.48x10^{-6}). A number of studies have found leptin to

have pro-mitogenic and anti-apoptotic effects in breast cancer cells (*34-37*). However, its effects on normal breast epithelial cells are less well characterized. Here, we treated both *BRCA1* and *BRCA2* heterozygous MCF-10A cells with leptin (400ng/mL) for 24 hours and found a significant induction of DNA damage in both cell lines (**Fig. 4D**) and in primary breast epithelial cells (**Fig. 4E**). Additionally, the ability of CM derived from women with obesity to induce DNA damage in *BRCA1* heterozygous breast epithelial cells is blocked when treating in the presence of a leptin neutralizing antibody (**Fig. 4F**).

Next, having identified insulin as positively correlated with DNA damage in tissue microarrays from *BRCA* mutation carriers, independent of BMI (**Fig. 1G, Table 2**), and as a top upstream regulator of gene expression in primary breast epithelial organoids isolated from women with BMI ≥25 (**Table 3**), we conducted additional mechanistic studies to determine whether insulin can directly induce DNA damage. Treatment of *BRCA1* and *BRCA2* heterozygous knockout MCF-10A cells with insulin (100nM) for 24 hours resulted in a significant increase in DNA damage in both cell lines (**Fig. 4G**) and in primary breast epithelial cells (**Fig. 4H**). Both leptin and insulin have been shown to act via PI3K (*38, 39*). Treatment of *BRCA1* heterozygous breast epithelial cells with a PI3K inhibitor, BKM120 (1μM), was effective at reducing the ability of CM derived from women with obesity to induced DNA damage (**Fig. 4I**). These data show that factors produced locally by breast adipose tissue from women with obesity or factors elevated with metabolic dysfunction contribute to induction of DNA damage in *BRCA* heterozygous knockout breast epithelial cells.

The effects of breast adipose conditioned media on DNA damage and repair in breast epithelial cells are dependent on a heterozygous *BRCA* mutation

RNA-seq was performed on *BRCA1*+/- MCF-10A cells treated with a subset of CM samples derived from women with a BMI < 25 or BMI ≥ 30 (n=3/group). Results demonstrate that consistent with DNA damage measurements (**Fig. S3A**), IPA analysis of differentially regulated genes in the cells treated with CM from breast adipose tissue of women with a BMI ≥ 30 relative to BMI < 25 (**Table S5**) showed increased activation of functions associated with DNA damage and genomic instability including "Formation of micronuclei", "Chromosomal instability", and "Breakage of chromosomes" (**Table 4**). Alternatively, activation of functions associated with DNA repair were decreased, including "Repair of DNA" and "Checkpoint control" (**Table 4**). Among the 47 genes involved in "Repair of DNA" that were significantly regulated by CM derived from adipose tissue of women with obesity (BMI ≥30 CM), a number of genes involved in homologous recombination-mediated repair were downregulated, including *MRE11A*, *BRCA1*, *BRIP1*, *XRCC2*, *BRCA2*, and *RAD54L* (**Table S6**).

To determine if the effects of breast adipose CM derived from women with obesity are specific to *BRCA1* heterozygous epithelial cells, MCF-10A cells WT for *BRCA1* were treated with the same CM derived from women with BMI < 25 or BMI ≥ 30 (n=3/group), and changes in gene expression were evaluated by RNA-seq (**Table S7**). Unlike in the *BRCA1*+/- MCF-10A cells, CM from women with a BMI ≥ 30 did not significantly induce DNA damage in WT MCF-10A cells compared to BMI <25 CM (**Fig. S3**). Interestingly, IPA analysis of differentially regulated genes in cells treated with CM from women with a BMI ≥ 30 relative to BMI < 25 showed a number of overlapping changes in the top 50 regulated "Diseases and Functions" in both WT and *BRCA1*+/- MCF-10A cells (**Fig. 5A**). However, when filtering the "Diseases and Functions" to highlight pathways associated with DNA damage or DNA repair, the majority of

functions associated with these pathways are not significantly regulated in the WT MCF-10A, unlike what is observed in *BRCA1*+/- MCF-10A cells (**Fig. 5B**).

High-fat diet feeding is associated with elevated mammary gland DNA damage and early tumor penetrance in female *Brca1* heterozygous knockout mice

DNA damage is a known driver of chromosomal defects that can lead to cancer. However, whether the obesity-associated elevation in breast epithelial cell DNA damage is linked to breast cancer penetrance in the setting of a heterozygous *BRCA* mutation has not been established. To investigate this question, we conducted preclinical studies utilizing mice that were developed to carry a whole-body heterozygous loss in *Brca1* (*Brca1*+/-) on a C57Bl/6 background. Four-week-old female *Brca1*+/- mice were randomized to receive low-fat diet (LFD) or high-fat diet (HFD) for 22 weeks to produce lean and obese mice, respectively (**Fig. 6A**). Mice fed HFD gained significantly more weight than LFD fed mice and weighed on average 34.1g vs 23.3g, respectively, at the time of euthanasia (**Fig. 6B**). Overall adiposity was also increased in association with HFD feeding as determined by greater accumulation of subcutaneous and visceral fat compared to the LFD group (**Fig. S4)**. To confirm that the HFD-fed mice exhibit altered metabolic homeostasis in our *Brca1*+/- model of diet-induced obesity, glucose tolerance tests were conducted after 21 weeks on experimental diets, highlighting delayed clearance of glucose from blood over 90 minutes post-intraperitoneal injection of glucose in the HFD group compared to LFD-fed mice (**Fig. 6C & D**). To determine whether changes observed in the mammary fat pad of *Brca1*+/- mice in response to feeding were analogous to those seen in the breast tissue of women in relation to obesity, RNA-seq was conducted on inguinal mammary fat pads from LFD and HFD mice harvested at euthanasia

(**Table S8**). IPA was used to identify activation of the top differentially regulated canonical pathways in HFD mammary fat pads relative to LFD, results of which were juxtaposed with regulation of these same pathways in human breast tissue from *BRCA* mutation carriers with BMI ≥ 25 vs BMI < 25 . The top 20 canonical pathways regulated by obesity in the mouse mammary fat pad show very similar regulation patterns compared to human breast tissue from women with overweight/obesity (BMI ≥ 25) (**Fig. 6E**), suggesting that diet-induced obesity in our *Brca1*+/- mice can serve as a model system for obesity in women carrying a *BRCA* mutation with respect to studies of the breast.

Similar to findings made in human breast tissue from *BRCA* mutation carriers, IF staining for γH2AX of *Brca1*+/- mouse mammary glands at euthanasia show that HFD-fed mice have elevated levels of mammary gland DNA damage compared to LFD-fed mice (**Fig. 6F**). Furthermore, there is a trend for a positive correlation between DNA damage and bodyweight (irrespective of diet) (**Fig. 6G**) and a significant positive correlation between DNA damage and mammary fat pad weight (**Fig. 6H)**, suggesting that level of adiposity may be a stronger predictor of DNA damage in mammary epithelium compared to whole body weight.

Next, we examined whether elevation in mammary gland DNA damage is associated with tumorigenesis. Female *Brca1*+/- mice were first made obese by HFD feeding for 10 weeks and then were implanted with a subcutaneous medroxyprogesterone acetate (MPA) pellet to sensitize them to mammary tumor development upon exposure to three doses of the carcinogen 7,12-dimethylbenz[a]anthracene (DMBA) (**Fig. 6I**). Mammary tumors developed earlier in the HFD group compared with the control LFD group (**Fig. 6J**). Additionally, 85.7% of mice in the HFD group developed mammary tumors by the end of the 28-week surveillance period compared to 69.2% of mice in the LFD group (**Fig. 6K**).

Elevated BMI is associated with DNA damage in the fallopian tube, but not ovary, of *BRCA* mutation carriers

In addition to elevated breast cancer risk, women carrying a *BRCA1* or *BRCA2* mutation have high lifetime risk for developing ovarian cancer (*1, 2*). Since weight gain is associated with increased risk of ovarian cancer in *BRCA* mutation carriers (*40*), we extended our studies in the breast to investigate the impact of elevated BMI on DNA damage in the ovarian epithelium as well as in epithelial cells of the fallopian tube. IF staining for γH2AX was performed with nuclear counter stain Hoechst to quantify number of foci of DNA damage per epithelial cell in non-tumorous ovarian tissue and fallopian tube fimbria from women carrying a *BRCA1* or *BRCA2* mutation undergoing prophylactic salpingo-oophorectomy. In the ovarian epithelium, there was no increase in DNA damage in the cases with overweight/obesity (n=9) compared to the cases with healthy weight (n=17) (**Fig. 7A**, *P*=0.59). However, there was a significant increase in DNA damage observed in the epithelial cells of the fallopian tube from women with overweight/obesity (n=12) compared to women with healthy weight (n=21) (**Fig. 7B**, *P*=0.03).

DISCUSSION

The data presented here demonstrate that BMI is positively associated with the accumulation of DNA double-strand breaks in normal breast epithelial cells in carriers of a mutation in *BRCA1* or *BRCA2*. Beyond BMI, insulin and insulin resistance, as measured by HOMA2 IR, were independently associated with DNA damage, irrespective of BMI or age. Accordingly, it is possible that *BRCA* mutation carriers who are defined as healthy weight by BMI, but are hyperinsulinemic (‘metabolically obese’), may also be at risk for elevated levels of

DNA damage and consequently, breast cancer development. Although previous studies have shown that inflammation can lead to DNA damage in both normal and cancerous cells in other tissues (*41-44*), our data do not support a link between local or systemic inflammation and breast epithelial cell DNA damage.

To our knowledge, this is the first study to conduct transcriptional profiling of non-cancerous breast tissue and isolated breast epithelial cells from *BRCA* mutation carriers with overweight/obesity vs those with healthy weight. While several factors and pathways associated with metabolic dysfunction were shown to be upregulated in breast tissue and in epithelial cells, the identification of pathways related to estrogen biosynthesis (tissue) and signaling (epithelial cells) were of particular interest given the availability of clinically approved drugs that target estrogen. Additionally, previous *in vitro* studies showed that treatment with estrogen and estrogen metabolites induced DNA damage in *BRCA1* heterozygous breast epithelial cells (*45*), providing further rationale for exploring the role of estrogen as a mediator of obesity-induced DNA damage. Here, we show that fulvestrant, an estrogen receptor degrader, is effective at reducing epithelial cell DNA damage in breast tissue explants from *BRCA* mutation carriers. However, this drug is not currently approved for use in the prevention setting and the side effects may limit its future use for this purpose. Alternatively, metformin is widely prescribed in patients with type II diabetes and has an excellent safety profile which makes this drug an intriguing option for preventative use in *BRCA* mutation carriers with excess bodyweight. We show that metformin was effective at reducing breast epithelial cell DNA damage at clinically relevant concentrations primarily due to effects on the breast adipose microenvironment. Previous studies have shown that metformin decreases adipose stromal cell expression of aromatase through activation of AMPK (*31, 32*). Our study extends these findings by demonstrating the

downstream consequence of downregulation in aromatase through mass spectrometry studies which showed marked reduction in E2 in breast tissue after metformin treatment. In addition to reducing estrogen exposure, previous work has shown that metformin treatment reduces endogenous reactive oxygen species (ROS) and associated DNA damage in a mammary epithelial cell line (*46*), providing an additional possible mechanism for the effects of metformin in our studies.

Epidemiological studies have reported decreased risk of breast cancer in *BRCA* mutation carriers in association with reduced estrogen exposure achieved via salpingo-oophorectomy surgery which diminishes ovarian estrogen production or through treatment with tamoxifen, an estrogen receptor antagonist in the breast (*47-49*). Our studies propose estrogen-mediated induction of DNA damage as a possible explanation for the protective effects observed by decreasing estrogen exposure in this population. Estrogen can induce DNA damage through various actions as reviewed by our group and others (*50, 51*), including through ligand binding to ERα which stimulates proliferation and potentially replication stress with ROS production as a byproduct of increased cellular respiration. Additionally, the metabolism of estrogen yields genotoxic metabolites, a process which produces ROS through redox cycling. These metabolites can directly interact with DNA to form adducts in an ER-independent manner. Given the multiple avenues through which estrogen can induced DNA damage in cells, additional studies are warranted to characterize the mechanisms of estrogen-induced DNA damage in breast epithelial cells from *BRCA* mutation carriers in the setting of obesity.

We also offer insights into potential mechanisms leading to DNA damage accumulation. Interestingly, our RNA-seq analysis of *BRCA1* heterozygous MCF-10A cells treated with breast adipose CM from women with obesity relative to CM from women with healthy weight not only

showed increased activation of pathways associated with DNA damage, but also downregulation of pathways associated with DNA repair. This raises the possibility that obesity may affect DNA repair capacity, which would be especially detrimental in cells already exhibiting defective DNA repair due to a mutation in *BRCA1* or *BRCA2*. In support of this possibility, MCF-10A cells WT for *BRCA* did not exhibit increased DNA damage when treated with CM from women with obesity, nor was there a significant impact on pathways associated with DNA damage or repair. This is consistent with our tissue microarray findings showing no association between BMI and breast epithelial cell DNA damage in age-matched non-mutation carriers. It is possible that DNA damage resolution occurs more quickly in cells that are WT for *BRCA*, and that we are not capturing the full extent of potential detrimental effects of obesity in this population. Nevertheless, our data suggest that the impact of overweight/obesity is distinct in *BRCA* mutation carriers compared with non-carriers with respect to DNA damage and repair. Therefore, although obesity is associated with increased breast cancer risk in post-menopausal women in the general population (*3*), the mechanisms that drive this risk are likely to be different than the possible mechanisms highlighted in our studies of *BRCA* mutation carriers, which will have implications on selection of effective risk reduction strategies in these two populations.

Our *in vitro* studies demonstrate the ability of several obesity-associated factors, including leptin and insulin, to cause the accumulation of DNA damage, suggesting a collective milieu of factors that may contribute to the elevation in DNA damage observed in *BRCA* mutation carriers in association with BMI. The ability of CM derived from women with obesity to induce damage in *BRCA1* heterozygous cells was diminished when treating in the presence of an antibody or drug that inhibits leptin or insulin signaling, respectively. Of note, since insulin signals through phosphatidylinositol 3-kinases (PI3K), we utilized BKM120, a PI3K inhibitor, to

disrupt insulin actions in the presence of CM. It is possible that inhibiting PI3K signaling is not only disrupting insulin signaling, but also signaling of other factors associated with obesity that act through PI3K, including growth factors or leptin, which collectively contributed to the observed decrease in DNA damage. Additionally, growing evidence points to a role for the PI3K pathway in the DNA damage response, however, these studies have been limited to cancer cells (*52-55*).

Our studies also show a link between obesity-induced DNA damage and tumor development using a *Brca1*+/- mouse model of diet-induced obesity. HFD-fed mice exhibited elevated mammary gland DNA damage in association with decreased latency and increased overall penetrance of mammary tumors when exposed to the carcinogen DMBA. These data suggest that the elevation in DNA damage that we observed in association with BMI in women carrying a *BRCA* mutation may also be associated with increased breast cancer penetrance. The extent to which data from this mouse model can be extrapolated to humans is somewhat limited given that we employed a carcinogen-indued tumor model, whereas in *BRCA* mutation carriers, tumors will arise after years of exposure to both endogenous and environmental factors, some of which will act as carcinogens.

Finally, our data show that obesity-associated DNA damage may not only be limited to the breast epithelium of *BRCA* mutation carriers. Although no increase in DNA damage was found in epithelial cells of the ovary in women with overweight/obesity undergoing prophylactic salpingo-oophorectomy, we did observe significantly higher levels of DNA damage in the epithelial cells of the fallopian tube in association with overweight/obesity. Our results are consistent with reports from recent years which point to the fallopian tube as the likely site of origin of ovarian cancer (*56, 57*), to be confirmed by ongoing clinical trials of risk-reducing

salpingectomy with delayed oophorectomy, and also highlights a potential mechanism for the link between weight gain and ovarian cancer in this population.

A limitation of our study includes a cohort size of n=69 in our correlation study of DNA damage and BMI which prevented us from analyzing effects of BMI separately in *BRCA1* and *BRCA2* mutation carriers. Although both BRCA1 and BRCA2 are essential for DNA repair, their roles in the DNA damage response are not identical and each mutation is associated with different subtypes of tumor development. Larger studies assessing the relative effect of BMI on DNA damage in *BRCA1* and *BRCA2* mutation carriers separately could provide additional information to help personalize risk estimates. Additionally, levels of estrogens vary considerably during the menstrual cycle and impact proliferation of breast epithelial cells. Our studies did not account for phase of menstrual cycle when assessing DNA damage which may have led to increased variability in our data, particularly considering our identification of estrogen as a mediator of obesity-induced epithelial cell DNA damage.

Many methodological challenges exist which explain the lack of consensus in epidemiological studies attempting to ascertain modifiers of breast cancer risk in *BRCA* mutation carriers, as reviewed by Milne & Antinou (*58*). Although a number of studies have associated bodyweight with increased risk of breast cancer as discussed earlier, the largest study to date to contradict these findings showed protective effects of BMI on pre-menopausal breast cancer risk in *BRCA* mutation carriers (*11*). Drawing definitive conclusions from this study is limited due to the utilization of subject-reported BMI at the time of study questionnaire which is subject to recall bias and utilization of calculated genetic BMI score which does not necessarily predict actual observed BMI and may be influenced by dietary and environmental factors. Additionally, a subset of the population with overweight/obesity may have received treatment for obesity-

associated co-morbidities like diabetes which potentially confounds risk assessment if these treatments or medications reduce breast cancer risk. Overall, given the inconsistencies in reported data and significant challenges in assessing modifiers of breast cancer risk in this population, the consensus to date is that there is insufficient evidence to determine the effect of bodyweight on breast cancer risk in *BRCA* mutation carriers (*58-60*). Therefore, a strength of our study is the presentation of mechanistic experimental evidence which helps to elucidate the relationship between bodyweight and breast cancer risk in this population.

Additionally, our findings provide rationale for conducting clinical trials in *BRCA* mutation carriers with overweight/obesity to test the efficacy of pharmacological interventions that target metabolic health, weight and/or estrogens. In fact, identifying which obesity-related factors need to be targeted for risk reduction, if not all, will have a meaningful impact on developing effective risk reduction strategies. Although recently reported results of the phase 3 randomized MA.32 trial (NCT01101438) found that addition of metformin to standard of care in non-diabetic patients with high-risk breast cancer did not significantly improve invasive disease-free survival vs placebo (*61*), it remains to be determined if metformin in the preventative setting would be effective at reducing risk of breast cancer, particularly among *BRCA* mutation carriers and those with metabolic dysfunction. Our studies point towards the potential of metformin in this setting, as it has been shown to reduce weight, as well as cause decreases in circulating levels of insulin, leptin and estrogens (*62-64*). These studies would help clarify whether accumulation of DNA damage over time is reversable or if targeted interventions prevent accumulation of further damage. Positive results would offer clinicians actionable evidence-based prevention strategies for patients in this high-risk population who opt to delay or forgo risk-reducing surgery.

MATERIALS AND METHODS

Study Design

The objective of this study was to gain insight into the role of obesity and metabolic dysfunction on breast cancer penetrance among carriers of germline mutations in *BRCA1* and *BRCA2* and to identify clinically relevant prevention strategies. Clinical samples including both archival tissues and prospectively collected tissues from *BRCA* mutation carriers and non-mutation carriers, as well as cell lines engineered to carry a *BRCA1* or *BRCA2* heterozygous knockout mutation and *Brca1*+/- mouse models were utilized in support of this objective. All studies utilizing human tissues were conducted in accordance with protocols approved by the Institutional Review Boards of Memorial Sloan Kettering Cancer Center (MSKCC) under protocol #10-040 and Weill Cornell Medicine under protocols #1510016712, 1004010984-01, 1612017836 and 20-01021391. Informed consent from each subject was obtained by study investigators prior to tissue collection. Animal experiments were conducted in accordance with an approved Institutional Animal Care and Use Committee protocol (#2018-0058) at Weill Cornell Medicine.

Studies utilizing archival tissues were coded and DNA damage was analyzed in a blinded fashion. Studies utilizing prospectively collected tissues and *in vitro* treatment studies were not blinded, however, DNA damage was analyzed by immunofluorescence staining using methodology to limit bias as described in the section "*Confocal microscopy & quantification of γH2AX foci*" below. Sample size power calculations were performed for human breast tissue microarray construction (BMI vs DNA damage study) and in animal studies. Any sample exclusion criteria are described in the sections below or in the figure legends.

Human breast tissue microarray construction & study population

Archival paraffin blocks of embedded non-tumorous breast tissue were obtained from 69 women carrying a *BRCA1* (n=40) or *BRCA2* (n=29) mutation and an age-matched subset of women WT for a *BRCA* mutation (n=17) who had previously undergone prophylactic or therapeutic mastectomy at MSKCC from 2011-2016. **Table 1** describes the clinical characteristics of the *BRCA* mutation carrier study population which were extracted from electronic medical records. BMI was calculated using height and weight recorded prior to surgery (kg/m^2) and menopausal status was determined per criteria established by the National Comprehensive Cancer Network (*65*). A pathologist reviewed hematoxylin & eosin-stained sections from each block to identify areas enriched in breast epithelium. Cores measuring 1.5mm in diameter from identified epithelial areas of each case were incorporated into paraffin blocks for the construction of tissue microarrays. Each tissue microarray was constructed with cases representing an equal distribution of clinical characteristics, including *BRCA1* or *BRCA2* mutation status and BMI. Unstained sections were cut from each tissue microarray and used for quantification of breast epithelial cell DNA damage by immunofluorescence staining as described in the section below.

Assessment of DNA damage by immunofluorescence staining

To quantify epithelial cell DNA damage, immunofluorescence staining of the DNA double strand break marker γH2AX was conducted on human tissue sections, mouse mammary gland tissue sections, or plated cells. Antibodies/reagents that were used include: primary γH2AX (p Ser139) antibody (Novus Biologicals #NB100-74435 unless otherwise stated) at

1:300 dilution, Goat anti-Mouse Alexa Fluor 546 secondary antibody (Life technologies #A11030) at 1:1000 dilution, Hoechst 33342 nuclear stain (Santa Cruz Biotechnology #SC-495790) at 1:1000 dilution, CAS block (Life Technologies #008120), M.O.M (Mouse-on-Mouse) immunodetection kit (Vector Laboratories # BMK-2202), and ProLong Gold Antifade Mountant (Invitrogen # P36934). Full staining procedures for tissue sections, plated cells, and co-localization studies can be found in the **Supplementary Materials**.

Confocal microscopy & quantification of γH2AX foci

Tissue slides or plated epithelial cells stained with γH2AX and Hoechst were imaged using a Zeiss LSM 880 confocal microscope. Confocal settings were not changed across samples within each experiment. Areas to image were first selected based on identification of regions rich in breast epithelial cells as determined by Hoechst staining prior to viewing the γH2AX channel to limit any potential bias in image selection. Images were exported to the image analysis software Imaris (Oxford Instruments) for semi-automated quantification of γH2AX foci per 100 cells. Imaris analysis settings were programmed to identify and quantify total cell number in each image and to identify number of γH2AX foci co-localizing with nuclei. All Imaris-analyzed images were visually inspected by investigators to ensure appropriate identification of γH2AX foci and exclusion of background staining. A minimum of 100 cells per case or condition were analyzed and DNA damage was reported as # of γH2AX foci per 100 cells unless stated otherwise. Any sample with less than 100 cells detected were excluded.

Quantification of blood biomarkers

Fasting blood was collected from patients prior to surgery. Serum was separated by centrifugation, aliquoted, and stored at -80°C. Enzyme-linked immunosorbent assay was used to measure serum levels of insulin (Mercodia, Uppsala, Sweden), hsCRP, glucose, SHBG, and IL-6 (R&D Systems, Minneapolis, MN) following the manufacturer's protocols.

RNA-Seq studies & computational analysis:

RNA-Sequencing (RNA-seq) was conducted on samples in 4 studies including: breast tissue from *BRCA* mutation carriers, isolated breast epithelial organoids from *BRCA* mutation carriers and non-carriers, breast adipose tissue conditioned media (CM)-treated *BRCA1* heterozygous or WT MCF-10A cells, and *Brca1*+/- mouse mammary fat pads. Details on RNA extraction, sequencing methodology, and computational analyses can be found in the **Supplementary Materials**.

Isolation of primary breast epithelial cells and breast explant studies

For *ex vivo* tissue explant studies and isolation of breast epithelial cells, breast tissue was obtained from women undergoing breast mammoplasty or mastectomy surgeries at Weill Cornell Medicine and MSKCC from 2017-2021. Surgical specimens were transferred from the operating room to a pathologist who evaluated the breast tissue to confirm that the tissue distributed for experimentation was normal and uninvolved with any quadrant where a tumor may have been present. The tissue was then brought to the laboratory and utilized in the experiments as described below.

Isolation of breast epithelial cells

Approximately 25mL of breast tissue was utilized in each organoid preparation with care taken dissect out overly fibrous areas or visible blood vessels. The tissue was finely minced and mixed with complete Ham's F12 media (Corning #10-080-CV, supplemented with 10% FBS and 1% penicillin/streptomycin) containing a digestion mix of 10mg/mL collagenase type 1 (Sigma Aldrich #C0130) and 10µg/mL hyaluronidase (Sigma Aldrich #H3506) in a total volume of 50mL. The tissue was digested overnight on a rotator at 37°C and then centrifuged. The supernatant containing free lipid and adipocytes was discarded and the pellet was washed and reconstituted in media followed by incubation at 4°C for 1 hour to ensure inhibition of enzyme activities. After centrifugation, the pellet was treated with red cell lysis buffer (Sigma Aldrich #11814389001), re-pelleted, reconstituted in media, and then ran through a 100µM filter followed by 40µM filter. Breast epithelial organoids were collected from the top of the 40µM filter in mammary epithelial cell growth medium with added supplements (PromoCell #C-21010). Isolated mammary epithelial organoids were snap frozen in liquid nitrogen for RNA extraction and RNA-sequencing or plated for *in vitro* studies.

Ex vivo metformin and fulvestrant explant studies

To examine the role of breast adipose tissue estrogen in mediation of DNA damage in *BRCA* mutant epithelial cells, breast explants were treated with drugs targeting estrogen signaling (fulvestrant) or production (metformin). 1 cm breast tissue explants were cut from breast tissue transferred after surgery and were plated in replicate in a 12-well dish. Metformin studies: Breast explants from n=3 subjects were cultured in complete Ham's F12 media (10% FBS, 1% penicillin/streptomycin) supplemented with either vehicle (methanol) or metformin

hydrochloride (25-100µM, Sigma #PHR1084). Fulvestrant studies: Breast explants from n=7 subjects were cultured in basal mammary epithelial cell growth media + 0.1% BSA containing either vehicle (ethanol) or 100uM fulvestrant (Sigma #I4409).

After 24 hours of treatment at 37°C in a 5% CO_2 incubator, explants were snap frozen in liquid nitrogen or formalin fixed and paraffin embedded. Tissue sections were cut from each paraffin block for assessment of breast epithelial cell DNA damage by immunofluorescence staining.

Collection of breast adipose tissue conditioned media

Conditioned media (CM) was generated from breast tissue obtained from n=36 women with BMIs that range from healthy weight to obese (20.6 – 49.1 kg/m^2). Ten 1 cm explant pieces of breast adipose tissue were cut from each case with a focus on fatty areas containing no visible blood vessels. The pieces were weighed and placed on a 10cm dish with 10mL of basal (phenol red free, serum free, and supplement mix free) mammary epithelial cell growth media (PromoCell #C-21215) containing 0.1% BSA. The explants were incubated at 37°C for 24 hours. After incubation the breast adipose tissue CM was collected and centrifuged at 300xg. The supernatant was aliquoted and stored at -80°C for use in *in vitro* treatment studies. Control CM consisted of the same collection media with the absence of conditioning by adipose explants.

In vitro studies in MCF-10A cells

Non-cancerous breast epithelial cell line MCF-10A carrying a *BRCA1* heterozygous mutation (185delAG/+) or WT for a *BRCA* mutation were purchased from Horizon Discovery and have been previously described (*66*). MCF-10A cells carrying a *BRCA2* heterozygous

mutation (6174insT/+) were generated in-house using CRISPR/Cas9 gene editing (additional details provided in the **Supplementary Materials**). Cells were cultured in DMEM/F12 (Invitrogen #11330-032) supplemented with 5% FBS, 1% penicillin/streptomycin and the following growth factors: 20ng/mL EGF, 0.5mg/mL hydrocortisone, 100ng/mL cholera toxin, and 10µg/mL insulin (all purchased from Sigma Aldrich). Cells were serum starved for 16 hours prior to treatments.

In CM studies, CM was thawed on ice from each case and diluted to a final concentration of 25% CM. In leptin studies, cells were treated with 400ng/mL of human recombinant leptin (Sigma #L4146). In leptin neutralization studies, obese CM was pre-incubated with a leptin neutralizing antibody (Lep ab, 13.3µg/mL, Fisher Scientific #AF398) for 1 hour at 4°C and then cells were treated with healthy weight or obese CM alone or obese CM + Lep ab. In insulin studies, cells were treated with 100nM insulin (Sigma #I1882). To block insulin signaling, cells were pre-treated with the PI3K inhibitor BKM120 (1uM, MedChemExpress #HY-70063) for 1 hour and then treated with obese CM + BKM120. All treatments were conducted in replicates or triplicates for 24 hours unless otherwise stated. After treatment, all wells were fixed with ice cold methanol followed by γH2AX IF staining.

***Brca1+/-* mouse studies**

Generation of Brca1+/- mice

To determine if obesity impacts mammary gland DNA damage and tumor penetrance in the setting of a *Brca* mutation, *Brca1* heterozygous (*Brca1*+/-) mice were generated on a C57BL/6 background as described in the **Supplementary Materials**.

Diet-induced obesity & mammary gland DNA damage

At 4 weeks of age, 24 female *Brca1*+/- mice were randomized to one of two groups (n=12/gp). One group was fed 10 kcal% low-fat diet (LFD, 12450Bi, Research Diets) and the second group was fed 60 kcal% high-fat diet (HFD, D12492i, Research Diets) *ad libitum* for 22 weeks until sacrifice. One week prior to sacrifice all mice were fasted overnight for 12 hours and underwent glucose tolerance tests to confirm obesity-induced metabolic dysfunction. In brief, baseline glucose measurements were taken from tail vein blood drop collection using a handheld glucose meter (Bayer Contour). Mice then received an intraperitoneal injection of 1g/kg glucose and tail vein blood glucose levels were recorded at 15-30 minute intervals over 90 minutes. Following the final measurement, respective experimental diets were re-started *ad libitum* for an additional week prior to sacrifice. Mice were euthanized via CO_2 inhalation and mammary gland tissue was collected and snap frozen (inguinal fat pads) for RNA-seq or fixed (thoracic fat pads) in 10% neutral buffered formalin overnight prior to paraffin embedding and sectioning for histological assessment of DNA damage.

MPA/DMBA tumor model

To investigate how obesity impacts mammary gland tumor development in *Brca1*+/- mice the same diet-induced obesity model as described above was utilized. At 4 weeks of age, 27 female *Brca1*+/- mice were randomized to one of two groups (n=13-14/gp). One group was fed LFD and the second group was fed HFD for the duration of the study. At 14 weeks of age (after 10 weeks on experimental diets) all mice were surgically implanted with a 40mg medroxyprogesterone acetate (MPA) pellet (90-day continuous release, Innovative Research of America, #NP-161) placed subcutaneously. At 15, 16, and 17 weeks of age all mice were dosed

with 1mg/22g bodyweight of the carcinogen 7,12-dimethylbenz[a]anthracene (DMBA) delivered by oral gavage in corn oil once per week for 3 consecutive weeks. Mammary tumor development and growth were monitored weekly by palpating all 5 mammary gland pairs and recording tumor presence and size with caliper measurements for 28 weeks following the last dose of DMBA. Mice were euthanized at the end of the 28-week surveillance period or earlier based on ethical endpoints, including tumor burden reaching 1.5cm. Mice that did not recover from pellet implantation surgery or displayed morbidity unrelated to mammary tumors were excluded from the study.

Quantitative steroid analysis in breast explants

Quantification of steroid levels (E2, E1, testosterone, and androstenedione) in snap frozen breast adipose tissue explants treated with metformin was performed using gas chromatography-mass spectrometry (GC-MS)-based steroid profiling as previously described (*67, 68*). Detailed protocol included in the **Supplementary Materials**.

Statistical analysis

To assess significant differences in baseline clinical characteristics and categorical variables the Fisher exact test was used. To test the strength of correlation between DNA damage and continuous variables, nonparametric Spearman's rank correlation coefficient was used with two-tailed *P* value to determine significance of correlations. A multivariable linear model was used to test the association between the level of DNA damage and clinical characteristics adjusting for BMI or age. Two-tailed Mann Whitney test was performed on clinical data testing significant differences between two groups. Two-tailed student's t-test was used on *in vitro*

761 treatment studies and in mouse studies comparing two groups. All results were performed using
762 R (version 4.0.5) or GraphPad Prism 9. Results with a *P*-value < 0.05 were considered
763 statistically significant.

764

765 **Supplementary Materials**

766 Materials and Methods

767 **Fig. S1.** Elevated BMI is associated with distinct changes in gene expression in breast epithelial
768 cells isolated from women who are WT for *BRCA* compared with breast epithelial cells from
769 *BRCA* mutation carriers

770 **Fig. S2.** Representative confocal images of γH2AX foci immunofluorescence staining in
771 *BRCA1*+/- and *BRCA2*+/- MCF-10A cells

772 **Fig. S3.** Breast adipose conditioned media from women with BMI ≥ 30 stimulates more DNA
773 damage in *BRCA1*+/- MCF-10A cells compared to conditioned media from women with BMI <
774 25.

775 **Fig. S4.** *Brca1*+/- mice fed high-fat diet have significantly greater accumulation of body fat
776 compared to *Brca1*+/- mice fed low-fat diet

777 **Fig. S5.** Generation of MCF-10A cells carrying a *BRCA2* heterozygous mutation

778 **Table S6.** Genes involved in "Repair of DNA" significantly regulated in *BRCA1*+/- MCF-10A
779 cells treated with breast adipose CM derived from women with obesity compared to women with
780 healthy weight

781 **Data file S1:** Tables S1-5 and S7-8: Full list of differentially expressed genes in presented RNA-
782 seq studies (multi-tab Excel file).

Data file S2: Original data for experiments presented

References (*69-80*)

References

1. K. B. Kuchenbaecker, J. L. Hopper, D. R. Barnes, K.-A. Phillips, T. M. Mooij, M.-J. Roos-Blom, S. Jervis, F. E. Van Leeuwen, R. L. Milne, N. Andrieu, D. E. Goldgar, M. B. Terry, M. A. Rookus, D. F. Easton, A. C. Antoniou, L. Mcguffog, D. G. Evans, D. Barrowdale, D. Frost, J. Adlard, K.-R. Ong, L. Izatt, M. Tischkowitz, R. Eeles, R. Davidson, S. Hodgson, S. Ellis, C. Nogues, C. Lasset, D. Stoppa-Lyonnet, J.-P. Fricker, L. Faivre, P. Berthet, M. J. Hooning, L. E. Van Der Kolk, C. M. Kets, M. A. Adank, E. M. John, W. K. Chung, I. L. Andrulis, M. Southey, M. B. Daly, S. S. Buys, A. Osorio, C. Engel, K. Kast, R. K. Schmutzler, T. Caldes, A. Jakubowska, J. Simard, M. L. Friedlander, S.-A. Mclachlan, E. Machackova, L. Foretova, Y. Y. Tan, C. F. Singer, E. Olah, A.-M. Gerdes, B. Arver, H. Olsson, Risks of Breast, Ovarian, and Contralateral Breast Cancer for BRCA1 and BRCA2 Mutation Carriers. *JAMA* **317**, 2402-2416 (2017).
2. S. Chen, G. Parmigiani, Meta-Analysis of BRCA1 and BRCA2 Penetrance. *Journal of Clinical Oncology* **25**, 1329-1333 (2007).
3. B. Lauby-Secretan, C. Scoccianti, D. Loomis, Y. Grosse, F. Bianchini, K. Straif, Body Fatness and Cancer — Viewpoint of the IARC Working Group. *New England Journal of Medicine* **375**, 794-798 (2016).

4. M. C. King, J. H. Marks, J. B. Mandell, G. New York Breast Cancer Study, Breast and ovarian cancer risks due to inherited mutations in BRCA1 and BRCA2. *Science* **302**, 643-646 (2003).
5. J. Kotsopoulos, O. I. Olopade, P. Ghadirian, J. Lubinski, H. T. Lynch, C. Isaacs, B. Weber, C. Kim-Sing, P. Ainsworth, W. D. Foulkes, A. Eisen, P. Sun, S. A. Narod, Changes in body weight and the risk of breast cancer in BRCA1 and BRCA2mutation carriers. *Breast Cancer Research* **7**, (2005).
6. E. Bruno, A. Oliverio, A. Paradiso, A. Daniele, S. Tommasi, D. A. Terribile, A. Filippone, M. Digennaro, B. Pilato, K. Danza, D. Guarino, C. Rossi, M. M. Rossi, E. Venturelli, M. Giussani, B. Peissel, P. Pasanisi, Lifestyle Characteristics in Women Carriers of BRCA Mutations: Results From an Italian Trial Cohort. *Clin Breast Cancer* **21**, e168-e176 (2021).
7. A. Nkondjock, A. Robidoux, Y. Paredes, S. A. Narod, P. Ghadirian, Diet, lifestyle and BRCA-related breast cancer risk among French-Canadians. *Breast Cancer Res Treat* **98**, 285-294 (2006).
8. S. Abbas, A. Siddique, N. Shahid, R. T. Khan, W. Fatima, Breast cancer risk associated with BRCA1/2 variants in the Pakistani population. *Breast Cancer* **26**, 365-372 (2019).
9. P. Manders, A. Pijpe, M. J. Hooning, I. Kluijt, H. F. Vasen, N. Hoogerbrugge, C. J. van Asperen, H. Meijers-Heijboer, M. G. Ausems, T. A. van Os, E. B. Gomez-Garcia, R. M. Brohet, Hebon, F. E. van Leeuwen, M. A. Rookus, Body weight and risk of breast cancer in BRCA1/2 mutation carriers. *Breast Cancer Res Treat* **126**, 193-202 (2011).
10. S. J. Kim, T. Huzarski, J. Gronwald, C. F. Singer, P. Møller, H. T. Lynch, S. Armel, B. Y. Karlan, W. D. Foulkes, S. L. Neuhausen, L. Senter, A. Eisen, C. Eng, S. Panchal, T.

Pal, O. Olopade, D. Zakalik, J. Lubinski, S. A. Narod, J. Kotsopoulos, P. Ainsworth, L. Bordeleau, N. Tung, E. Friedman, W. Meschino, C. Snyder, K. Metcalfe, E. Warner, B. Rosen, R. Demsky, J. N. Weitzel, K. Panabaker, F. Couch, S. Manoukian, B. Pasini, M. B. Daly, L. Steele, H. Saal, T. Fallen, M. Wood, W. Mckinnon, E. Lemire, A. E. Chudley, K. Serfas, C. Elser, S. T. Vadaparampil, O. Ginsburg, C. A. Cullinane, J. L. Blum, T. Ross, C. Mauer, A. Kwong, C. Cybulski, J. Mccuaig, D. Rayson, C. Isaacs, Prospective evaluation of body size and breast cancer risk among BRCA1 and BRCA2 mutation carriers. *International Journal of Epidemiology* **47**, 987-997 (2018).

11. F. Qian, S. Wang, J. Mitchell, L. Mcguffog, D. Barrowdale, G. Leslie, J. C. Oosterwijk, W. K. Chung, D. G. Evans, C. Engel, K. Kast, C. M. Aalfs, M. A. Adank, J. Adlard, B. A. Agnarsson, K. Aittomäki, E. Alducci, I. L. Andrulis, B. K. Arun, M. G. E. M. Ausems, J. Azzollini, E. Barouk-Simonet, J. Barwell, M. Belotti, J. Benitez, A. Berger, A. Borg, A. R. Bradbury, J. Brunet, S. S. Buys, T. Caldes, M. A. Caligo, I. Campbell, S. M. Caputo, J. Chiquette, K. B. M. Claes, J. Margriet Collée, F. J. Couch, I. Coupier, M. B. Daly, R. Davidson, O. Diez, S. M. Domchek, A. Donaldson, C. M. Dorfling, R. Eeles, L. Feliubadaló, L. Foretova, J. Fowler, E. Friedman, D. Frost, P. A. Ganz, J. Garber, V. Garcia-Barberan, G. Glendon, A. K. Godwin, E. B. Gómez Garcia, J. Gronwald, E. Hahnen, U. Hamann, A. Henderson, C. B. Hendricks, J. L. Hopper, P. J. Hulick, E. N. Imyanitov, C. Isaacs, L. Izatt, Á. Izquierdo, A. Jakubowska, K. Kaczmarek, E. Kang, B. Y. Karlan, C. M. Kets, S.-W. Kim, Z. Kim, A. Kwong, Y. Laitman, C. Lasset, M. Hyuk Lee, J. Won Lee, J. Lee, J. Lester, F. Lesueur, J. T. Loud, J. Lubinski, N. Mebirouk, H. E. J. Meijers-Heijboer, A. Meindl, A. Miller, M. Montagna, T. M. Mooij, P. J. Morrison, E. Mouret-Fourme, K. L. Nathanson, S. L. Neuhausen, H. Nevanlinna, D. Niederacher, F.

C. Nielsen, R. L. Nussbaum, K. Offit, E. Olah, K.-R. Ong, L. Ottini, S. K. Park, P. Peterlongo, G. Pfeiler, C. M. Phelan, B. Poppe, N. Pradhan, P. Radice, S. J. Ramus, J. Rantala, M. Robson, G. C. Rodriguez, R. K. Schmutzler, C. G. Hutten Selkirk, P. D. Shah, J. Simard, C. F. Singer, J. Sokolowska, D. Stoppa-Lyonnet, C. Sutter, Y. Yen Tan, R. M. Teixeira, S. H. Teo, M. B. Terry, M. Thomassen, M. Tischkowitz, A. E. Toland, K. M. Tucker, N. Tung, C. J. Van Asperen, K. Van Engelen, E. J. Van Rensburg, S. Wang-Gohrke, B. Wappenschmidt, J. N. Weitzel, D. Yannoukakos, M. H. Greene, M. A. Rookus, D. F. Easton, G. Chenevix-Trench, A. C. Antoniou, D. E. Goldgar, O. I. Olopade, T. R. Rebbeck, D. Huo, Height and Body Mass Index as Modifiers of Breast Cancer Risk in BRCA1/2 Mutation Carriers: A Mendelian Randomization Study. *JNCI: Journal of the National Cancer Institute* **111**, 350-364 (2019).

12. S. M. Grundy, Obesity, Metabolic Syndrome, and Cardiovascular Disease. *The Journal of Clinical Endocrinology & Metabolism* **89**, 2595-2600 (2004).

13. K. Sun, C. M. Kusminski, P. E. Scherer, Adipose tissue remodeling and obesity. *Journal of Clinical Investigation* **121**, 2094-2101 (2011).

14. H. Sell, C. Habich, J. Eckel, Adaptive immunity in obesity and insulin resistance. *Nat Rev Endocrinol* **8**, 709-716 (2012).

15. P. Bhardwaj, K. A. Brown, Obese Adipose Tissue as a Driver of Breast Cancer Growth and Development: Update and Emerging Evidence. *Front Oncol* **11**, 638918 (2021).

16. K. A. Brown, Metabolic pathways in obesity-related breast cancer. *Nature Reviews Endocrinology* **17**, 350-363 (2021).

17. E. R. Simpson, S. R. Davis, Minireview: Aromatase and the Regulation of Estrogen Biosynthesis—Some New Perspectives. *Endocrinology* **142**, 4589-4594 (2001).

18. X. Wang, E. R. Simpson, K. A. Brown, Aromatase overexpression in dysfunctional adipose tissue links obesity to postmenopausal breast cancer. *The Journal of Steroid Biochemistry and Molecular Biology* **153**, 35-44 (2015).
19. H. Zahid, K. Subbaramaiah, N. M. Iyengar, X. K. Zhou, I. C. Chen, P. Bhardwaj, A. Gucalp, M. Morrow, C. A. Hudis, A. J. Dannenberg, K. A. Brown, Leptin regulation of the p53-HIF1alpha/PKM2-aromatase axis in breast adipose stromal cells: a novel mechanism for the obesity-breast cancer link. *Int J Obes (Lond)* **42**, 711-720 (2018).
20. F. Liu, J. He, H. Wang, D. Zhu, Y. Bi, Adipose Morphology: a Critical Factor in Regulation of Human Metabolic Diseases and Adipose Tissue Dysfunction. *Obesity Surgery* **30**, 5086-5100 (2020).
21. K. A. Brown, Metabolic pathways in obesity-related breast cancer. *Nat Rev Endocrinol* **17**, 350-363 (2021).
22. N. Marino, R. German, X. Rao, E. Simpson, S. Liu, J. Wan, Y. Liu, G. Sandusky, M. Jacobsen, M. Stoval, S. Cao, A. M. V. Storniolo, Upregulation of lipid metabolism genes in the breast prior to cancer diagnosis. *npj Breast Cancer* **6**, (2020).
23. K. Yoshida, Y. Miki, Role of BRCA1 and BRCA2 as regulators of DNA repair, transcription, and cell cycle in response to DNA damage. *Cancer Science* **95**, 866-871 (2004).
24. A. R. Venkitaraman, Cancer Susceptibility and the Functions of BRCA1 and BRCA2. *Cell* **108**, 171-182 (2002).
25. E. Kowalska, S. A. Narod, T. Huzarski, S. Zajaczek, J. Huzarska, B. Gorski, J. Lubinski, Increased Rates of Chromosome Breakage in BRCA1 Carriers Are Normalized by Oral

Selenium Supplementation. *Cancer Epidemiology, Biomarkers & Prevention* **14**, 1302-1306 (2005).

26. M. Zaki, W. Basha, H. T. El-Bassyouni, S. El-Toukhy, T. Hussein, Evaluation of DNA damage profile in obese women and its association to risk of metabolic syndrome, polycystic ovary syndrome and recurrent preeclampsia. *Genes Dis* **5**, 367-373 (2018).

27. C. M. Dungan, B. D. Peck, R. G. Walton, Z. Huang, M. M. Bamman, P. A. Kern, C. A. Peterson, In vivo analysis of γH2AX+ cells in skeletal muscle from aged and obese humans. *The FASEB Journal* **34**, 7018-7035 (2020).

28. J. Fieres, M. Fischer, C. Sauter, M. Moreno-Villanueva, A. Burkle, P. H. Wirtz, The burden of overweight: Higher body mass index, but not vital exhaustion, is associated with higher DNA damage and lower DNA repair capacity. *DNA Repair (Amst)* **114**, 103323 (2022).

29. V. S. Y. Tay, S. Devaraj, T. Koh, G. Ke, K. C. Crasta, Y. Ali, Increased double strand breaks in diabetic β-cells with a p21 response that limits apoptosis. *Scientific Reports* **9**, (2019).

30. P. G. Morris, C. A. Hudis, D. Giri, M. Morrow, D. J. Falcone, X. K. Zhou, B. Du, E. Brogi, C. B. Crawford, L. Kopelovich, K. Subbaramaiah, A. J. Dannenberg, Inflammation and Increased Aromatase Expression Occur in the Breast Tissue of Obese Women with Breast Cancer. *Cancer Prevention Research* **4**, 1021-1029 (2011).

31. K. A. Brown, N. I. Hunger, M. Docanto, E. R. Simpson, Metformin inhibits aromatase expression in human breast adipose stromal cells via stimulation of AMP-activated protein kinase. *Breast Cancer Research and Treatment* **123**, 591-596 (2010).

32. N. U. Samarajeewa, S. Ham, F. Yang, E. R. Simpson, K. A. Brown, Promoter-specific effects of metformin on aromatase transcript expression. *Steroids* **76**, 768-771 (2011).

33. H. D. Soule, T. M. Maloney, S. R. Wolman, W. D. Peterson, Jr., R. Brenz, C. M. McGrath, J. Russo, R. J. Pauley, R. F. Jones, S. C. Brooks, Isolation and characterization of a spontaneously immortalized human breast epithelial cell line, MCF-10. *Cancer Res* **50**, 6075-6086 (1990).

34. C. N. Perera, H. G. Chin, N. Duru, I. G. Camarillo, Leptin-regulated gene expression in MCF-7 breast cancer cells: mechanistic insights into leptin-regulated mammary tumor growth and progression. *Journal of Endocrinology* **199**, 221-233 (2008).

35. N. K. Saxena, P. M. Vertino, F. A. Anania, D. Sharma, Leptin-induced Growth Stimulation of Breast Cancer Cells Involves Recruitment of Histone Acetyltransferases and Mediator Complex to CYCLIN D1 Promoter via Activation of Stat3. *Journal of Biological Chemistry* **282**, 13316-13325 (2007).

36. A. L. Strong, J. F. Ohlstein, B. A. Biagas, L. V. Rhodes, D. T. Pei, H. A. Tucker, C. Llamas, A. C. Bowles, M. F. Dutreil, S. Zhang, J. M. Gimble, M. E. Burow, B. A. Bunnell, Leptin produced by obese adipose stromal/stem cells enhances proliferation and metastasis of estrogen receptor positive breast cancers. *Breast Cancer Research* **17**, (2015).

37. N. Yin, D. Wang, H. Zhang, X. Yi, X. Sun, B. Shi, H. Wu, G. Wu, X. Wang, Y. Shang, Molecular Mechanisms Involved in the Growth Stimulation of Breast Cancer Cells by Leptin. *Cancer Research* **64**, 5870-5875 (2004).

38. H.-K. Park, R. S. Ahima, Leptin signaling. *F1000Prime Reports* **6**, (2014).

39. B. D. Hopkins, M. D. Goncalves, L. C. Cantley, Insulin–PI3K signalling: an evolutionarily insulated metabolic driver of cancer. *Nature Reviews Endocrinology* **16**, 276-283 (2020).

40. S. J. Kim, J. Lubinski, T. Huzarski, P. Moller, S. Armel, B. Y. Karlan, L. Senter, A. Eisen, W. D. Foulkes, C. F. Singer, N. Tung, L. Bordeleau, S. L. Neuhausen, O. I. Olopade, C. Eng, J. N. Weitzel, R. Fruscio, S. A. Narod, J. Kotsopoulos, G. Hereditary Ovarian Cancer Clinical Study, Weight Gain and the Risk of Ovarian Cancer in BRCA1 and BRCA2 Mutation Carriers. *Cancer Epidemiol Biomarkers Prev* **30**, 2038-2043 (2021).

41. F. Colotta, P. Allavena, A. Sica, C. Garlanda, A. Mantovani, Cancer-related inflammation, the seventh hallmark of cancer: links to genetic instability. *Carcinogenesis* **30**, 1073-1081 (2009).

42. L. M. Coussens, Z. Werb, Inflammation and cancer. *Nature* **420**, 860-867 (2002).

43. L. B. Meira, J. M. Bugni, S. L. Green, C.-W. Lee, B. Pang, D. Borenshtein, B. H. Rickman, A. B. Rogers, C. A. Moroski-Erkul, J. L. Mcfaline, D. B. Schauer, P. C. Dedon, J. G. Fox, L. D. Samson, DNA damage induced by chronic inflammation contributes to colon carcinogenesis in mice. *Journal of Clinical Investigation*, (2008).

44. O. Kiraly, G. Gong, W. Olipitz, S. Muthupalani, B. P. Engelward, Inflammation-Induced Cell Proliferation Potentiates DNA Damage-Induced Mutations In Vivo. *PLOS Genetics* **11**, e1004901 (2015).

45. K. I. Savage, K. B. Matchett, E. M. Barros, K. M. Cooper, G. W. Irwin, J. J. Gorski, K. S. Orr, J. Vohhodina, J. N. Kavanagh, A. F. Madden, A. Powell, L. Manti, S. S. Mcdade, B. H. Park, K. M. Prise, S. A. Mcintosh, M. Salto-Tellez, D. J. Richard, C. T. Elliott, D. P.

965 Harkin, BRCA1 Deficiency Exacerbates Estrogen-Induced DNA Damage and Genomic
966 Instability. *Cancer Research* **74**, 2773-2784 (2014).
967 46. C. Algire, O. Moiseeva, X. Deschênes-Simard, L. Amrein, L. Petruccelli, E. Birman, B.
968 Viollet, G. Ferbeyre, M. N. Pollak, Metformin Reduces Endogenous Reactive Oxygen
969 Species and Associated DNA Damage. *Cancer Prevention Research* **5**, 536-543 (2012).
970 47. N. D. Kauff, S. M. Domchek, T. M. Friebel, M. E. Robson, J. Lee, J. E. Garber, C.
971 Isaacs, D. G. Evans, H. Lynch, R. A. Eeles, S. L. Neuhausen, M. B. Daly, E. Matloff, J.
972 L. Blum, P. Sabbatini, R. R. Barakat, C. Hudis, L. Norton, K. Offit, T. R. Rebbeck, Risk-
973 Reducing Salpingo-Oophorectomy for the Prevention of BRCA1- and BRCA2-
974 Associated Breast and Gynecologic Cancer: A Multicenter, Prospective Study. *Journal of*
975 *Clinical Oncology* **26**, 1331-1337 (2008).
976 48. S. A. Narod, J. S. Brunet, P. Ghadirian, M. Robson, K. Heimdal, S. L. Neuhausen, D.
977 Stoppa-Lyonnet, C. Lerman, B. Pasini, P. de los Rios, B. Weber, H. Lynch, G. Hereditary
978 Breast Cancer Clinical Study, Tamoxifen and risk of contralateral breast cancer in
979 BRCA1 and BRCA2 mutation carriers: a case-control study. Hereditary Breast Cancer
980 Clinical Study Group. *Lancet* **356**, 1876-1881 (2000).
981 49. T. R. Rebbeck, H. T. Lynch, S. L. Neuhausen, S. A. Narod, L. Van'T Veer, J. E. Garber,
982 G. Evans, C. Isaacs, M. B. Daly, E. Matloff, O. I. Olopade, B. L. Weber, Prophylactic
983 Oophorectomy in Carriers of BRCA1 or BRCA2 Mutations. *New England Journal of*
984 *Medicine* **346**, 1616-1622 (2002).
985 50. C. E. Caldon, Estrogen Signaling and the DNA Damage Response in Hormone
986 Dependent Breast Cancers. *Frontiers in Oncology* **4**, (2014).

51. P. Bhardwaj, C. C. Au, A. Benito-Martin, H. Ladumor, S. Oshchepkova, R. Moges, K. A. Brown, Estrogens and breast cancer: Mechanisms involved in obesity-related development, growth and progression. *The Journal of Steroid Biochemistry and Molecular Biology* **189**, 161-170 (2019).

52. T. T. Huang, E. J. Lampert, C. Coots, J. M. Lee, Targeting the PI3K pathway and DNA damage response as a therapeutic strategy in ovarian cancer. *Cancer Treat Rev* **86**, 102021 (2020).

53. A. Juvekar, H. Hu, S. Yadegarynia, C. A. Lyssiotis, S. Ullas, E. C. Lien, G. Bellinger, J. Son, R. C. Hok, P. Seth, M. B. Daly, B. Kim, R. Scully, J. M. Asara, L. C. Cantley, G. M. Wulf, Phosphoinositide 3-kinase inhibitors induce DNA damage through nucleoside depletion. *Proc Natl Acad Sci U S A* **113**, E4338-4347 (2016).

54. R. J. Cardnell, Y. Feng, L. Diao, Y. H. Fan, F. Masrorpour, J. Wang, Y. Shen, G. B. Mills, J. D. Minna, J. V. Heymach, L. A. Byers, Proteomic markers of DNA repair and PI3K pathway activation predict response to the PARP inhibitor BMN 673 in small cell lung cancer. *Clin Cancer Res* **19**, 6322-6328 (2013).

55. A. Juvekar, L. N. Burga, H. Hu, E. P. Lunsford, Y. H. Ibrahim, J. Balmana, A. Rajendran, A. Papa, K. Spencer, C. A. Lyssiotis, C. Nardella, P. P. Pandolfi, J. Baselga, R. Scully, J. M. Asara, L. C. Cantley, G. M. Wulf, Combining a PI3K inhibitor with a PARP inhibitor provides an effective therapy for BRCA1-related breast cancer. *Cancer Discov* **2**, 1048-1063 (2012).

56. J. Ducie, F. Dao, M. Considine, N. Olvera, P. A. Shaw, R. J. Kurman, I.-M. Shih, R. A. Soslow, L. Cope, D. A. Levine, Molecular analysis of high-grade serous ovarian

carcinoma with and without associated serous tubal intra-epithelial carcinoma. *Nature Communications* **8**, (2017).

57. S. I. Labidi-Galy, E. Papp, D. Hallberg, N. Niknafs, V. Adleff, M. Noe, R. Bhattacharya, M. Novak, S. Jones, J. Phallen, C. A. Hruban, M. S. Hirsch, D. I. Lin, L. Schwartz, C. L. Maire, J.-C. Tille, M. Bowden, A. Ayhan, L. D. Wood, R. B. Scharpf, R. Kurman, T.-L. Wang, I.-M. Shih, R. Karchin, R. Drapkin, V. E. Velculescu, High grade serous ovarian carcinomas originate in the fallopian tube. *Nature Communications* **8**, (2017).

58. R. L. Milne, A. C. Antoniou, Modifiers of breast and ovarian cancer risks for BRCA1 and BRCA2 mutation carriers. *Endocrine-Related Cancer* **23**, T69-T84 (2016).

59. T. M. Friebel, S. M. Domchek, T. R. Rebbeck, Modifiers of Cancer Risk in BRCA1 and BRCA2 Mutation Carriers: A Systematic Review and Meta-Analysis. *JNCI: Journal of the National Cancer Institute* **106**, dju091-dju091 (2014).

60. A. M. Coletta, S. K. Peterson, L. A. Gatus, K. J. Krause, S. M. Schembre, S. C. Gilchrist, B. Arun, Y. N. You, M. A. Rodriguez-Bigas, L. L. Strong, K. H. Lu, K. Basen-Engquist, Diet, weight management, physical activity and Ovarian & Breast Cancer Risk in women with BRCA1/2 pathogenic Germline gene variants: systematic review. *Hereditary Cancer in Clinical Practice* **18**, (2020).

61. P. J. Goodwin, B. E. Chen, K. A. Gelmon, T. J. Whelan, M. Ennis, J. Lemieux, J. A. Ligibel, D. L. Hershman, I. A. Mayer, T. J. Hobday, J. M. Bliss, P. Rastogi, M. Rabaglio-Poretti, S. D. Mukherjee, J. R. Mackey, V. G. Abramson, C. Oja, R. Wesolowski, A. M. Thompson, D. W. Rea, P. M. Stos, L. E. Shepherd, V. Stambolic, W. R. Parulekar, Effect of Metformin vs Placebo on Invasive Disease–Free Survival in Patients With Breast Cancer. *JAMA* **327**, 1963 (2022).

62. P. J. Goodwin, R. J. O. Dowling, M. Ennis, B. E. Chen, W. R. Parulekar, L. E. Shepherd, M. J. Burnell, R. Vander Meer, A. Molckovsky, A. Gurjal, K. A. Gelmon, J. A. Ligibel, D. L. Hershman, I. A. Mayer, T. J. Whelan, T. J. Hobday, P. Rastogi, M. Rabaglio-Poretti, J. Lemieux, A. M. Thompson, D. W. Rea, V. Stambolic, Effect of metformin versus placebo on metabolic factors in the MA.32 randomized breast cancer trial. *NPJ Breast Cancer* **7**, 74 (2021).

63. P. J. Goodwin, W. R. Parulekar, K. A. Gelmon, L. E. Shepherd, J. A. Ligibel, D. L. Hershman, P. Rastogi, I. A. Mayer, T. J. Hobday, J. Lemieux, A. M. Thompson, K. I. Pritchard, T. J. Whelan, S. D. Mukherjee, H. I. Chalchal, C. D. Oja, K. S. Tonkin, V. Bernstein, B. E. Chen, V. Stambolic, Effect of metformin vs placebo on and metabolic factors in NCIC CTG MA.32. *J Natl Cancer Inst* **107**, (2015).

64. I. Pimentel, B. E. Chen, A. E. Lohmann, M. Ennis, J. Ligibel, L. Shepherd, D. L. Hershman, T. Whelan, V. Stambolic, I. Mayer, T. Hobday, J. Lemieux, A. Thompson, P. Rastogi, K. Gelmon, D. Rea, M. Rabaglio, S. Ellard, M. Mates, P. Bedard, L. Pitre, T. Vandenberg, R. J. O. Dowling, W. Parulekar, P. J. Goodwin, The Effect of Metformin vs Placebo on Sex Hormones in Canadian Cancer Trials Group MA.32. *J Natl Cancer Inst* **113**, 192-198 (2021).

65. W. J. Gradishar, B. O. Anderson, S. L. Blair, H. J. Burstein, A. Cyr, A. D. Elias, W. B. Farrar, A. Forero, S. H. Giordano, L. J. Goldstein, D. F. Hayes, C. A. Hudis, S. J. Isakoff, B. M. Ljung, P. K. Marcom, I. A. Mayer, B. McCormick, R. S. Miller, M. Pegram, L. J. Pierce, E. C. Reed, K. E. Salerno, L. S. Schwartzberg, M. L. Smith, H. Soliman, G. Somlo, J. H. Ward, A. C. Wolff, R. Zellars, D. A. Shead, R. Kumar, P. National

Comprehensive Cancer Network Breast Cancer, Breast cancer version 3.2014. *J Natl Compr Canc Netw* **12**, 542-590 (2014).

66. H. Konishi, M. Mohseni, A. Tamaki, J. P. Garay, S. Croessmann, S. Karnan, A. Ota, H. Y. Wong, Y. Konishi, B. Karakas, K. Tahir, A. M. Abukhdeir, J. P. Gustin, J. Cidado, G. M. Wang, D. Cosgrove, R. Cochran, D. Jelovac, M. J. Higgins, S. Arena, L. Hawkins, J. Lauring, A. L. Gross, C. M. Heaphy, Y. Hosokawa, E. Gabrielson, A. K. Meeker, K. Visvanathan, P. Argani, K. E. Bachman, B. H. Park, Mutation of a single allele of the cancer susceptibility gene BRCA1 leads to genomic instability in human breast epithelial cells. *Proc Natl Acad Sci U S A* **108**, 17773-17778 (2011).

67. S. Han, T. Baba, S. Yanai, D. J. Byun, K. I. Morohashi, J. H. Kim, M. H. Choi, GC-MS-based metabolic signatures reveal comparative steroidogenic pathways between fetal and adult mouse testes. *Andrology* **9**, 400-406 (2021).

68. J. Y. Moon, K. M. McNamara, J. J. Lee, B. C. Chung, H. Sasano, M. H. Choi, Improved detectability of sex steroids from frozen sections of breast cancer tissue using GC-triple quadrupole-MS. *J Steroid Biochem Mol Biol* **178**, 185-192 (2018).

69. N. L. Bray, H. Pimentel, P. Melsted, L. Pachter, Near-optimal probabilistic RNA-seq quantification. *Nat Biotechnol* **34**, 525-527 (2016).

70. M. I. Love, W. Huber, S. Anders, Moderated estimation of fold change and dispersion for RNA-seq data with DESeq2. *Genome Biol* **15**, 550 (2014).

71. A. Dobin, C. A. Davis, F. Schlesinger, J. Drenkow, C. Zaleski, S. Jha, P. Batut, M. Chaisson, T. R. Gingeras, STAR: ultrafast universal RNA-seq aligner. *Bioinformatics* **29**, 15-21 (2013).

72. H. Li, B. Handsaker, A. Wysoker, T. Fennell, J. Ruan, N. Homer, G. Marth, G. Abecasis, R. Durbin, S. Genome Project Data Processing, The Sequence Alignment/Map format and SAMtools. *Bioinformatics* **25**, 2078-2079 (2009).

73. C. Trapnell, A. Roberts, L. Goff, G. Pertea, D. Kim, D. R. Kelley, H. Pimentel, S. L. Salzberg, J. L. Rinn, L. Pachter, Differential gene and transcript expression analysis of RNA-seq experiments with TopHat and Cufflinks. *Nat Protoc* **7**, 562-578 (2012).

74. T. Derrien, R. Johnson, G. Bussotti, A. Tanzer, S. Djebali, H. Tilgner, G. Guernec, D. Martin, A. Merkel, D. G. Knowles, J. Lagarde, L. Veeravalli, X. Ruan, Y. Ruan, T. Lassmann, P. Carninci, J. B. Brown, L. Lipovich, J. M. Gonzalez, M. Thomas, C. A. Davis, R. Shiekhattar, T. R. Gingeras, T. J. Hubbard, C. Notredame, J. Harrow, R. Guigo, The GENCODE v7 catalog of human long noncoding RNAs: analysis of their gene structure, evolution, and expression. *Genome Res* **22**, 1775-1789 (2012).

75. X. Liu, H. Holstege, H. van der Gulden, M. Treur-Mulder, J. Zevenhoven, A. Velds, R. M. Kerkhoven, M. H. van Vliet, L. F. Wessels, J. L. Peterse, A. Berns, J. Jonkers, Somatic loss of BRCA1 and p53 in mice induces mammary tumors with features of human BRCA1-mutated basal-like breast cancer. *Proc Natl Acad Sci U S A* **104**, 12111-12116 (2007).

76. H. Liu, C. J. Murphy, F. A. Karreth, K. B. Emdal, F. M. White, O. Elemento, A. Toker, G. M. Wulf, L. C. Cantley, Identifying and Targeting Sporadic Oncogenic Genetic Aberrations in Mouse Models of Triple-Negative Breast Cancer. *Cancer Discov* **8**, 354-369 (2018).

77. F. Schwenk, U. Baron, K. Rajewsky, A cre-transgenic mouse strain for the ubiquitous deletion of loxP-flanked gene segments including deletion in germ cells. *Nucleic Acids Res* **23**, 5080-5081 (1995).

78. A. Katti, M. Foronda, J. Zimmerman, B. Diaz, M. P. Zafra, S. Goswami, L. E. Dow, GO: a functional reporter system to identify and enrich base editing activity. *Nucleic Acids Res* **48**, 2841-2852 (2020).

79. M. P. Zafra, E. M. Schatoff, A. Katti, M. Foronda, M. Breinig, A. Y. Schweitzer, A. Simon, T. Han, S. Goswami, E. Montgomery, J. Thibado, E. R. Kastenhuber, F. J. Sanchez-Rivera, J. Shi, C. R. Vakoc, S. W. Lowe, D. F. Tschaharganeh, L. E. Dow, Optimized base editors enable efficient editing in cells, organoids and mice. *Nat Biotechnol* **36**, 888-893 (2018).

80. J. Y. Moon, K. M. McNamara, J. J. Lee, B. C. Chung, H. Sasano, M. H. Choi, Improved detectability of sex steroids from frozen sections of breast cancer tissue using GC-triple quadrupole-MS. *J Steroid Biochem Mol Biol* **178**, 185-192 (2018).

Acknowledgments:

We thank Dr. David Otterburn and Dr. Leslie Cohen, Department of Surgery, and Dr. Paula Ginter, Department of Pathology, at Weill Cornell Medicine for facilitating access to reduction mammoplasty tissue. Studies were conducted with the support and facilities provided by the Microscopy and Image Analysis Core Facility, Genomics Resources Core Facility, Center for Translational Pathology, and the Research Animal Resource Center at Weill Cornell Medicine (New York, NY). All schematics were created in BioRender.

Funding:

National Cancer Institute of the National Institutes of Health grant 1R01CA215797 (KAB)

National Cancer Institute of the National Institutes of Health grant F31CA236306 (PB)

Anne Moore Breast Cancer Research Fund (KAB)

National Breast Cancer Foundation grant ECF-16-004 (KAB)

Emilie Lippmann and Janice Jacobs McCarthy Research Scholar Award in Breast Cancer (KAB)

National Center for Advancing Translational Sciences of the National Institutes of Health grant KL2-TR-002385 (MKF)

National Institute of General Medical Sciences of the National Institutes of Health grant T32GM007739 to the Weill Cornell/Rockefeller/Sloan Kettering Tri-Institutional MD-PhD Program (MA)

The content is solely the responsibility of the authors and does not necessarily represent the official views of the National Institutes of Health or other funding agencies.

Author contributions:

Conceptualization: KAB, NMI

Methodology: KAB, PB, NMI, HZ, DJB, MHO, QS, RB, MF, LED, DDG, XKZ

Investigation: PB, HZ, KMC, DJB, CL, CL, PP, MA, MF, SO, MP, BH, MKF

Formal analysis: KAB, PB, QS, OS, RB, XKZ

Resources: KAB, MHC, OE, AML, LHE, MM, JAS, LCC

Funding acquisition: KAB, PB

Project administration: KAB

Supervision: KAB

Writing – original draft: PB, KAB

Writing – review & editing: All authors

Competing interests:

NMI receives consulting fees from Novartis, Pfizer, and Seattle Genetics; Honoraria from Curio Science, Cardinal Health, OncLive, IntrinsiQ Health; Research funding (to institution) from Novartis, SynDevRx, National Cancer Institute, American Cancer Society, Breast Cancer Research Foundation, and the Conquer Cancer Foundation. LED is a scientific advisor and holds equity in Mirimus Inc. and has received consulting fees and/or honoraria from Volastra Therapeutics, Revolution Medicines, Repare Therapeutics, Fog Pharma, and Frazier Healthcare Partners. BDH is a founder and consultant for Faeth Therapeutics.

Data and materials availability:

All data for experiments presented in this paper are included in Data File S2 or in the Supplementary Materials. Full list of differentially expressed genes used in computational analyses from all RNA-seq studies presented are included in Data file S1. Requests for transfer of materials (e.g. cell line generated in this study) can be made by contacting the corresponding author.

Tables:

Table 1. Baseline characteristics of study population based on BMI category

Variables	All (n=69)	Healthy Weight (n=43)	Overweight/Obese (n=26)	*P*
BMI, median (range)	23.9 (19.38-44.9)	22.2 (19.38-24.7)	28.8 (25.3-44.9)	<0.001
BRCA mutation, n (%)				0.6
BRCA1	40 (58.0%)	26 (60.5%)	14 (53.8%)	
BRCA2	29 (42.0%)	17 (39.5%)	12 (46.2%)	
Age, median (range)	40 (25-69)	39.0 (25-60)	44.5 (28-69)	0.03
Diabetes, n (%)				0.4
No	68 (98.6%)	43 (100.0%)	25 (96.2%)	
Yes	1 (1.4%)	0 (0%)	1 (3.8%)	
Dyslipidemia, n (%)				0.01
No	62 (89.9%)	42 (97.7%)	20 (76.9%)	
Yes	7 (10.1%)	1 (2.3%)	6 (23.1%)	
Hypertension, n (%)				0.046
No	61 (88.4%)	41 (95.3%)	20 (76.9%)	
Yes	8 (11.6%)	2 (4.7%)	6 (23.1%)	
Menopausal status, n (%)				0.022
Pre-	46 (66.7%)	33 (76.7%)	13 (50.0%)	
Post-	23 (33.3%)	10 (23.3%)	13 (50.0%)	
Race, n (%)				0.1
Asian	1 (1.4%)	1 (2.3%)	0 (0.0%)	
Black	2 (2.9%)	2 (4.7%)	0 (0.0%)	
Other	2 (2.9%)	0 (0.0%)	2 (7.7%)	
White	56 (81.2%)	33 (76.7%)	23 (88.5%)	
Missing	8 (11.6%)	7 (16.3%)	1 (3.8%)	
Invasive tumor present, n (%)				0.7
No	39 (56.5%)	25 (58.1%)	14 (53.8%)	
Yes	30 (43.5%)	18 (41.9%)	12 (46.2%)	
Tumor subtype, n (%)				>0.9
HR+	22 (31.9%)	14 (32.6%)	8 (30.8%)	
HER2+	1 (1.4%)	1 (2.3%)	0 (0.0%)	
TNBC	9 (13.0%)	5 (11.6%)	4 (15.4%)	
N/A	37 (53.6%)	23 (53.5%)	14 (53.8%)	

Abbreviations: BMI, body mass index; HR, hormone receptor; HER2, human epidermal growth factor receptor 2; TNBC, triple negative breast cancer

Table 2. Association of clinical features and blood biomarkers with DNA damage, adjusting for age or BMI

Variables	Correction	*P*	Correction	*P*
BMI			Age	0.003
Age	BMI	0.335		
SHBG (nmol/L)	BMI	0.081	Age	0.020
Insulin (mU/L)	BMI	0.009	Age	<0.001
HOMA2 IR	BMI	0.010	Age	<0.001

Abbreviations: BMI, body mass index; SHBG, steroid hormone binding globulin, HOMA2 IR, homeostatic model assessment 2 for insulin resistance

Table 3. Predicted upstream regulators of gene expression differences in breast epithelial organoids isolated from *BRCA* mutation carriers with BMI ≥ 25 relative to carriers with BMI < 25 and associated gene expression in whole breast tissue

Organoid upstream regulator	Predicted activation state	Activation z-score	*P*-value of overlap	Breast tissue RNA-Seq	*P*-value
beta-estradiol	Activated	4.728	2.2E-10	see Fig. 2C	
IL2	Activated	3.402	3.1E-02	0.563	2.3E-01
GDF2	Activated	3.217	4.9E-03	-0.081	9.8E-01
IL15	Activated	3.152	1.5E-03	0.299	4.1E-05
TNFSF11	Activated	3.125	3.2E-02	-0.757	9.7E-02
Insulin	Activated	3.113	6.1E-03		
IL4	Activated	3.016	1.9E-03	-0.25	7.4E-01
TGFB1	Activated	2.942	6.0E-09	0.455	2.2E-08
hydrogen peroxide	Activated	2.839	3.1E-03		
IL3	Activated	2.674	7.6E-04	-0.122	9.7E-01
CSF1	Activated	2.602	8.9E-03	0.35	1.4E-06
Lh	Activated	2.598	1.7E-03		
dinoprost (PGF2α)	Activated	2.569	2.9E-02		
IL5	Activated	2.496	5.5E-03	0.173	6.9E-01
ATP	Activated	2.443	8.7E-03		
MDK	Activated	2.433	2.9E-02	-0.34	4.4E-03
AGT	Activated	2.345	4.2E-03	-0.56	9.6E-04
ANGPT2	Activated	2.329	1.1E-03	0.38	9.2E-05
WNT5A	Activated	2.292	1.7E-03	0.184	1.3E-01
pyruvic acid	Activated	2.156	1.5E-03		

Table 4. Activation of diseases or functions associated with DNA damage or DNA repair in *BRCA1*+/- epithelial cells treated with breast adipose tissue conditioned media derived from women with obesity relative to women with healthy weight

Categories	Diseases or functions annotation	*P*-value	Predicted activation state	Activation z-score	# Molecules
Cellular Assembly and Organization	Formation of micronuclei	2.53E-06	Increased	2.756	9
DNA Replication, Recombination & Repair	Chromosomal aberration	5.37E-06	Increased	2.853	31
	Chromosomal instability	2.43E-08	Increased	2.603	19
	Breakage of chromosomes	2.88E-05	Increased	2.488	11
Cell Cycle; DNA Replication, Recombination & Repair	Checkpoint control	1.99E-06	Decreased	-2.756	15
	Spindle checkpoint	9.33E-07	Decreased	-2.035	12
DNA Replication, Recombination & Repair	Repair of DNA	4.36E-09	Decreased	-3.334	47
	Double-stranded DNA break repair of tumor cell lines	9.94E-06	Decreased	-2.241	14
	Metabolism of DNA	2.10E-10	Decreased	-2.09	54

Figure Legends:

Fig. 1. BMI and additional clinical characteristics are positively correlated with DNA damage in breast epithelium of women carrying a *BRCA* mutation

(**A**) Representative image of tissue microarray section of normal breast epithelium shown by H&E stain (top) and by IF staining (bottom) for γH2AX (red, arrows) co-localizing with Hoechst (blue), scale bar=10μM. (**B**) Correlation between epithelial cell DNA damage as measured by #γH2AX foci/100 cells with BMI in *BRCA* mutation carriers and in (**C**) age-matched women WT for *BRCA*. (**D**) Correlation between epithelial cell DNA damage and age. (**E**) Average DNA

damage in the study population grouped by menopausal status: pre-menopausal, n=46 and post-menopausal, n=23. (**F-K**) Epithelial cell DNA damage correlated with circulating serum biomarkers in a subset of the study population with available fasting serum at the time of surgery (n=41). (**K**) Average DNA damage in the study population when grouped by those exhibiting histological breast adipose tissue inflammation defined as presence of crown-like structures (CLS) vs those with no CLS present (i.e. CLS- vs CLS+). Two-tailed Mann Whitney test was used to determine significant differences in grouped comparisons and data is presented as mean +/- SD. Correlation between variables were assessed by Spearman's rank correlation coefficient (ρ). Associated *P* value and ρ are shown for continuous variables with 95% confidence intervals. **P*<0.05; ns, not significant; n=69 unless otherwise stated.

Fig. 2. Elevated BMI is associated with significant changes in gene expression in breast adipose tissue and in breast epithelial cells of *BRCA* mutation carriers

(**A**) Unsupervised heatmap of whole breast tissue gene expression by RNA-seq in *BRCA* mutation carriers identified by BMI category of < 25 (n=64, blue) or ≥ 25 (n=67, pink). (**B**) IPA analysis of RNA-seq data showing activation (z-score) of the top 20 canonical pathways regulated in breast tissue from *BRCA* mutation carriers with BMI ≥ 25 compared to carriers with BMI < 25 with an absolute value z-score of >0.5. (**C**) Heatmap of RNA-seq gene expression data generated from breast tissue of *BRCA* mutation carriers grouped by BMI category of < 25 (yellow) or ≥ 25 (green) showing selected genes associated with estrogen biosynthesis, estradiol (E2) inactivation, and estrogen metabolism. Corresponding gene expression (log2FC) and *P* values are shown in tissue from women with BMI ≥ 25 relative to BMI < 25. (**D**) DNA damage in breast epithelial cells was quantified in tissue sections from n=61 patients from whom

corresponding whole breast tissue RNA-seq data was also available. The cases were stratified by quartile of DNA damage and the breast tissue gene expression from cases with the highest level of DNA damage (quartile 4, Q4) were compared to cases with the lowest level (quartile 1, Q1) of DNA damage. Top 15 canonical pathways regulated in Q4 vs Q1 with an absolute value z-score of >2.0 are shown. (**E**) Representative H&E-stained images of a breast tissue section before digestion and epithelial organoids after isolation are shown. Organoids stain positively for luminal marker cytokeratin 8 (CK8, green) and basal marker cytokeratin 14 (CK14, red) as shown by IF staining merged with Hoechst (blue). Scale bar= 50μM. (**F**) IPA analysis of RNA-seq gene expression data showing activation of the top 20 canonical pathways regulated in primary breast epithelial organoids from *BRCA* mutation carriers with BMI ≥ 25 (n=9) relative to carriers with BMI < 25 (n=10) with an absolute value z-score of >1.0.. The length of the bars on all canonical pathway graphs are determined by the Fisher's Exact Test *P* value with entities that have a -log(p-value) >1.3 shown.

Fig. 3. Targeting estrogen signaling or production in breast tissue decreases epithelial cell DNA damage in women carrying a mutation in *BRCA1* or *BRCA2*

(**A**) Representative IHC staining of ERα expression in breast epithelium from carriers of a *BRCA1* or *BRCA2* mutation (top panel). Representative IF staining showing co-localization of #γH2AX foci (green) with ERα positive cells (red) (bottom panel), scale bar=10μM. (**B**) Experimental schematic showing collection of breast tissue and plating of explants or isolation of primary breast epithelial organoids for treatment studies. (**C**) Breast epithelial cell DNA damage assessed by IF (#γH2AX foci/100 cells) in e*x vivo* breast adipose tissue explants from *BRCA* mutation carriers treated with fulvestrant (100nM) for 24 hours (pooled average of n=7 patients).

(**D**) Aromatase (CYP19A1) expression in breast tissue from *BRCA* mutation carriers (RNA-seq counts per million, CPM) correlated with level of breast epithelial cell DNA damage in corresponding tissue sections (n=58). Spearman's rank correlation coefficient (ρ) and associated *P* value are shown with 95% confidence intervals. (**E**) Breast epithelial cell DNA damage in e*x vivo* breast adipose tissue explants from *BRCA* mutation carriers treated with metformin (0-100μM) for 24 hours (pooled average of n=3 patients). (**F**) DNA damage in isolated primary breast epithelial cells from *BRCA* mutation carriers treated with metformin (0-100μM) for 24 hours (representative of n=2 experiments). (**G**) Average 17β-estradiol (E2) levels and (**H**) overlay of E2, testosterone (T), androstenedione, and estrone (E1) levels in e*x vivo* breast adipose explants after 24-hour treatment with metformin (pooled average of n=3 patients). Student's t-test was used to determine significant differences from control unless otherwise stated. Data is presented as mean +/- SEM. **P* <0.05, ***P* <0.01, ****P*<0.001.

Fig. 4. Obesity-induced changes to the local breast adipose microenvironment promotes DNA damage in *BRCA1* and *BRCA2* heterozygous breast epithelial cells

(**A**) Experimental schematic showing the collection of breast adipose tissue conditioned media (CM) from women with healthy weight and with overweight/obesity as defined by BMI. (**B**) MCF-10A cells were treated with CM for 24 hours. DNA damage assessed by IF (#γH2AX foci/100 cells) is shown correlated with BMI in *BRCA1*+/- (n=36 CM cases) and (**C**) *BRCA2*+/- (n=13 CM cases) MCF-10A cells. Blue dotted line represents level of DNA damage induced by control CM (media not conditioned by adipose explants). Spearman's rank correlation coefficient (ρ) and associated *P* value are shown along with 95% confidence intervals. (**D**) DNA damage in *BRCA1*+/- and *BRCA2*+/- MCF-10A cells and in (**E**) primary *BRCA1*+/- breast epithelial cells

treated with leptin (400ng/µl) for 24 hours. (**F**) DNA damage in *BRCA1*+/- MCF-10A cells after 24-hour treatment with CM derived from a woman with healthy weight ("Healthy CM"), with obesity ("ob CM"), or "ob CM" in the presence of a leptin neutralizing antibody (Lep Ab). (**G**) DNA damage in *BRCA1*+/- and *BRCA2*+/- MCF-10A cells and in (**H**) primary *BRCA2*+/- breast epithelial cells treated with insulin (100nM) for 24 hours. (**I**) DNA damage in *BRCA1*+/- MCF-10A cells after 24-hour treatment with "healthy CM", "ob CM", or "ob CM" in the presence of PI3K inhibitor BKM120 (1µM). Student's t-test was used to determine significant differences in (**D-I)**. All experiments in MCF-10A cells were conducted a minimum of two times with representative results from one experiment shown. Data in primary cells were generated from cells treated in triplicate. Data is presented as mean +/- SD. **P* <0.05, ***P* <0.01, ****P* <0.001, ns= not significant.

Fig. 5. Breast adipose CM from women with obesity regulates gene expression and pathways associated with DNA damage and repair more robustly in *BRCA1*+/- MCF-10A cells compared to WT MCF-10A cells

(**A**) MCF-10A cells carrying a heterozygous *BRCA1* mutation (*BRCA1*+/-) or WT for *BRCA* were treated with breast adipose CM from women with BMI ≥ 30 (n=3) or BMI < 25 (n=3) for 24 hours. RNA-seq was conducted followed by IPA analysis of differentially expressed genes in BMI ≥ 30 relative to BMI < 25 CM treated cells. Top 50 regulated "Diseases and Functions" are shown with corresponding activation z-score in *BRCA1*+/- vs WT cells. (**B**) Diseases and functions were filtered to show pathways involved in DNA damage and DNA repair. Activation z-scores are color coded as heatmaps with gradations of red representing a positive z-score and gradations blue representing a negative z-score. Significantly regulated pathways as defined by -

log(p-value) >1.3 are shown. Pathways with cells showing no color and a not applicable ("N/A") z-score are not significantly regulated.

Fig. 6. High-fat diet feeding leads to elevated mammary gland DNA damage in association with increased mammary tumor penetrance and decreased tumor latency in *Brca1*+/- mice

(**A**) Experimental schematic of diet-induced obesity in female *Brca1*+/- mice (n=12/gp). (**B**) Average body weight of mice fed low-fat diet (LFD) or high-fat diet (HFD) over 22 wks. (**C**) Glucose tolerance test conducted one week prior to sacrifice and (**D**) area under curve (AUC) calculation for each group (mean +/- SEM). (**E**) RNA-seq was conducted on whole mammary fat pad tissue from HFD and LFD mice (n=6/gp). Activation of top 20 canonical pathways regulated in mammary fat pads from HFD mice compared to LFD mice are shown adjacent to corresponding pathway regulation in breast tissue from *BRCA* mutation carriers with BMI ≥ 25 vs carriers with BMI <25 (n=64-67/gp). (**F**) DNA damage assessed by IF (#γH2AX foci/100 cells) in mammary glands at the time of sacrifice. (**G**) Correlation between mammary gland DNA damage and mouse body weight and (**H**) mammary fat pad weight among all mice. Spearman's rank correlation coefficient (ρ) and associated *P* values are shown along with 95% confidence intervals. (**I**) Experimental schematic of MPA/DMBA-induced tumorigenesis model in female *Brca1*+/- mice randomized to LFD or HFD groups (n=13-14/gp). (**J**) Mammary tumor development in LFD and HFD mice shown as % of mice tumor free over the 28-week surveillance period. (**K**) Overall mammary tumor penetrance at the end of the surveillance period shown as % of mice in each group that developed a mammary tumor. Student's t-test was used to determine significance unless otherwise stated. Data is presented as mean +/- SD unless otherwise stated. **P* <0.05.

Fig. 7. BMI is associated with DNA damage in the fallopian tube but not ovary

(**A**) DNA damage assessed by IF (#γH2AX foci/cell) in epithelial cells of the ovary and in (**B**) epithelial cells of fallopian tube fimbriae in *BRCA* mutation carriers grouped by BMI category of healthy weight (n=17-21/gp) or overweight (Ow)/obese (n=9-12). Two-tailed Mann Whitney test was used to determine significant differences (*P* value) between groups. Data is presented as mean +/-SEM.

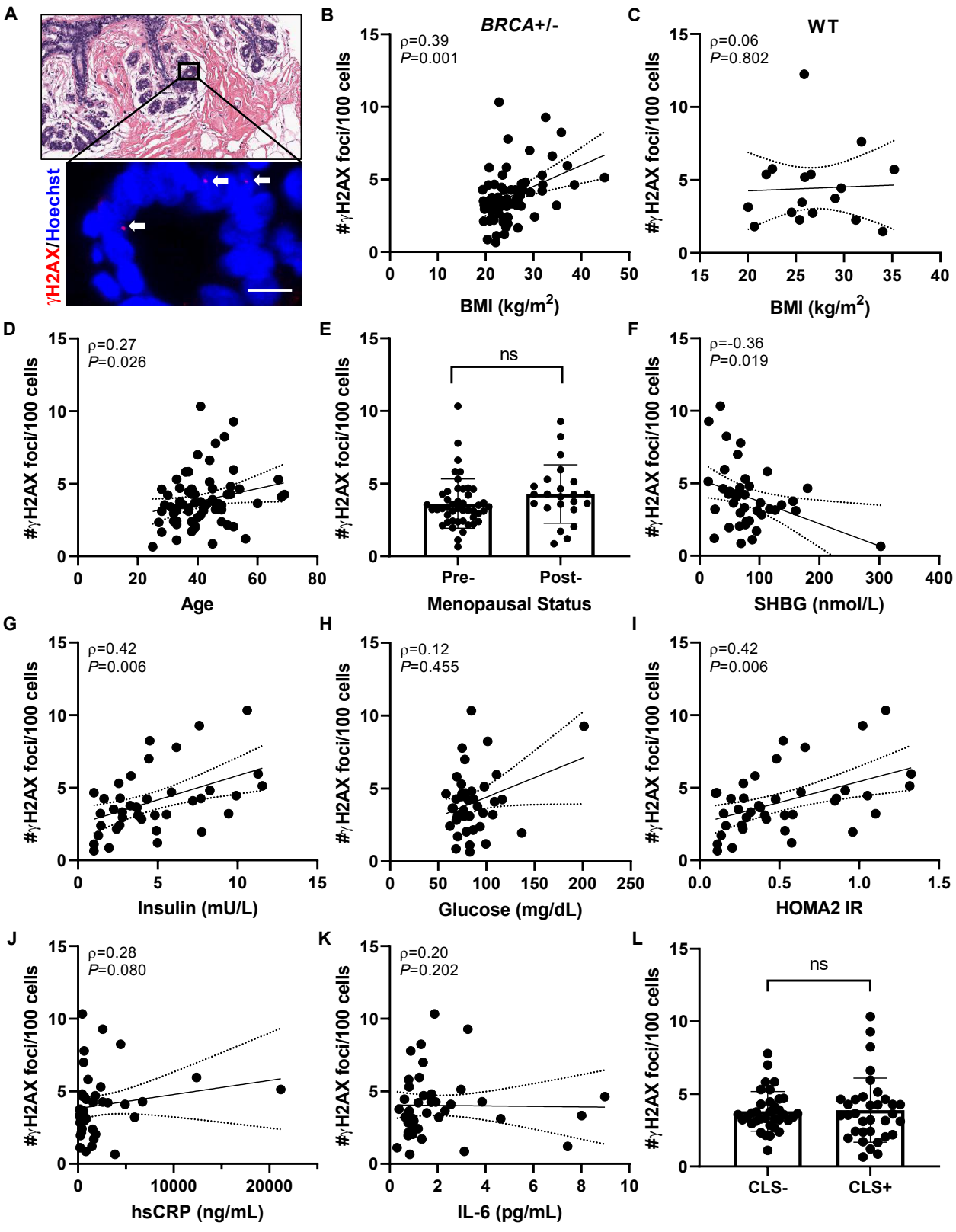
A
γH2AX/Hoechst
B
BRCA+/-
ρ=0.39
P=0.001
#γH2AX foci/100 cells
BMI (kg/m2)
C
WT
ρ=0.06
P=0.802
#γH2AX foci/100 cells
BMI (kg/m2)
D
ρ=0.27
P=0.026
#γH2AX foci/100 cells
Age
E
ns
#γH2AX foci/100 cells
Pre-
Post-
Menopausal Status
F
ρ=-0.36
P=0.019
#γH2AX foci/100 cells
SHBG (nmol/L)
G
ρ=0.42
P=0.006
#γH2AX foci/100 cells
Insulin (mU/L)
H
ρ=0.12
P=0.455
#γH2AX foci/100 cells
Glucose (mg/dL)
I
ρ=0.42
P=0.006
#γH2AX foci/100 cells
HOMA2 IR
J
ρ=0.28
P=0.080
#γH2AX foci/100 cells
hsCRP (ng/mL)
K
ρ=0.20
P=0.202
#γH2AX foci/100 cells
IL-6 (pg/mL)
L
ns
#γH2AX foci/100 cells
CLS-
CLS+

Fig.1

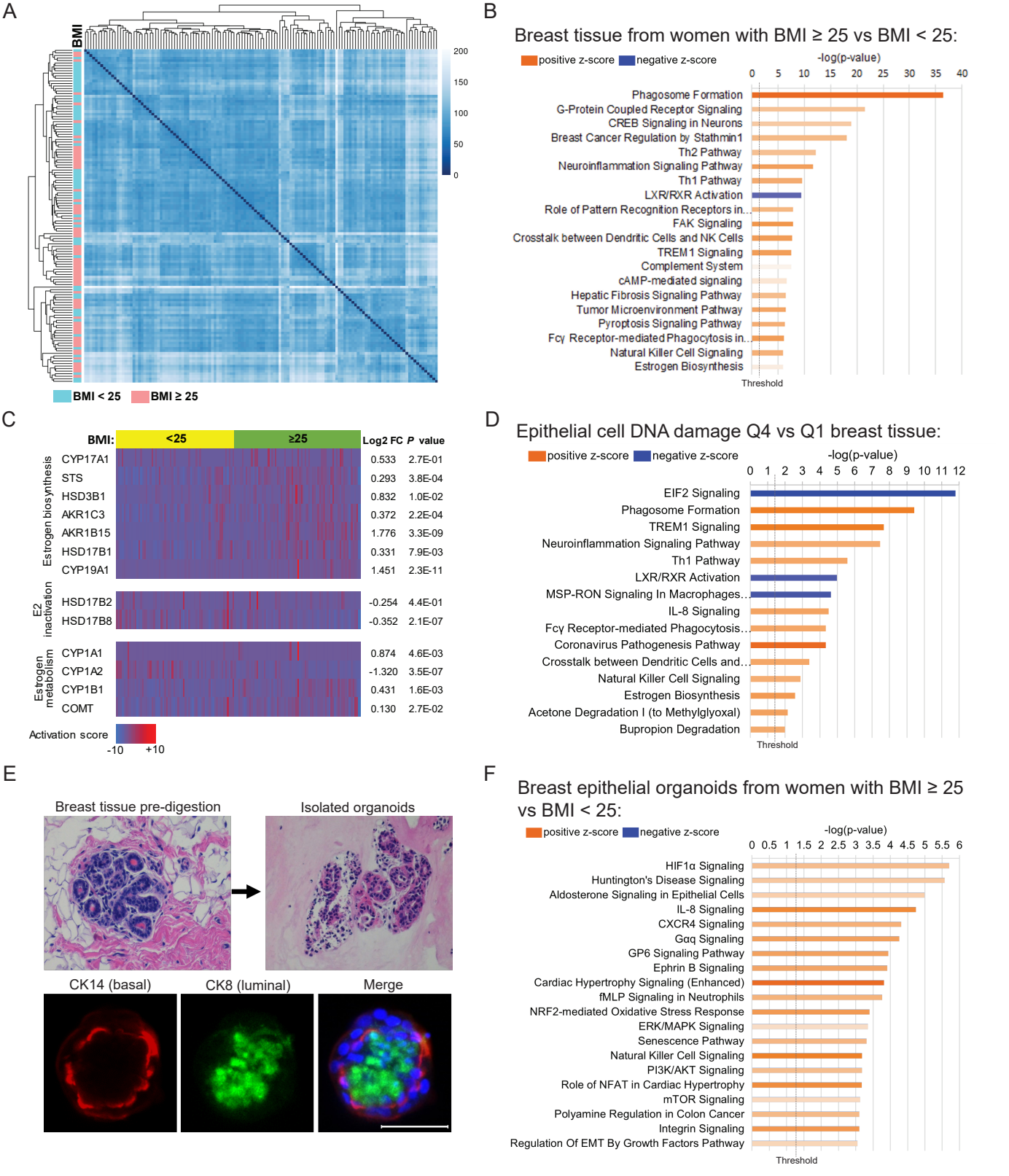
A
BMI
200
150
100
50
0
BMI < 25
BMI ≥ 25
B
Breast tissue from women with BMI ≥ 25 vs BMI < 25:
positive z-score
negative z-score
-log(p-value)
0 5 10 15 20 25 30 35 40
Phagosome Formation
G-Protein Coupled Receptor Signaling
CREB Signaling in Neurons
Breast Cancer Regulation by Stathmin1
Th2 Pathway
Neuroinflammation Signaling Pathway
Th1 Pathway
LXR/RXR Activation
Role of Pattern Recognition Receptors in...
FAK Signaling
Crosstalk between Dendritic Cells and NK Cells
TREM1 Signaling
Complement System
cAMP-mediated signaling
Hepatic Fibrosis Signaling Pathway
Tumor Microenvironment Pathway
Pyroptosis Signaling Pathway
Fcγ Receptor-mediated Phagocytosis in...
Natural Killer Cell Signaling
Estrogen Biosynthesis
Threshold
C
BMI:
<25
≥25
Log2 FC
P value
Estrogen biosynthesis
CYP17A1 0.533 2.7E-01
STS 0.293 3.8E-04
HSD3B1 0.832 1.0E-02
AKR1C3 0.372 2.2E-04
AKR1B15 1.776 3.3E-09
HSD17B1 0.331 7.9E-03
CYP19A1 1.451 2.3E-11
E2 inactivation
HSD17B2 -0.254 4.4E-01
HSD17B8 -0.352 2.1E-07
Estrogen metabolism
CYP1A1 0.874 4.6E-03
CYP1A2 -1.320 3.5E-07
CYP1B1 0.431 1.6E-03
COMT 0.130 2.7E-02
Activation score
-10
+10
D
Epithelial cell DNA damage Q4 vs Q1 breast tissue:
positive z-score
negative z-score
-log(p-value)
0 1 2 3 4 5 6 7 8 9 10 11 12
EIF2 Signaling
Phagosome Formation
TREM1 Signaling
Neuroinflammation Signaling Pathway
Th1 Pathway
LXR/RXR Activation
MSP-RON Signaling In Macrophages...
IL-8 Signaling
Fcγ Receptor-mediated Phagocytosis...
Coronavirus Pathogenesis Pathway
Crosstalk between Dendritic Cells and...
Natural Killer Cell Signaling
Estrogen Biosynthesis
Acetone Degradation I (to Methylglyoxal)
Bupropion Degradation
Threshold
E
Breast tissue pre-digestion
Isolated organoids
CK14 (basal)
CK8 (luminal)
Merge
F
Breast epithelial organoids from women with BMI ≥ 25 vs BMI < 25:
positive z-score
negative z-score
-log(p-value)
0 0.5 1 1.5 2 2.5 3 3.5 4 4.5 5 5.5 6
HIF1α Signaling
Huntington's Disease Signaling
Aldosterone Signaling in Epithelial Cells
IL-8 Signaling
CXCR4 Signaling
Gαq Signaling
GP6 Signaling Pathway
Ephrin B Signaling
Cardiac Hypertrophy Signaling (Enhanced)
fMLP Signaling in Neutrophils
NRF2-mediated Oxidative Stress Response
ERK/MAPK Signaling
Senescence Pathway
Natural Killer Cell Signaling
PI3K/AKT Signaling
Role of NFAT in Cardiac Hypertrophy
mTOR Signaling
Polyamine Regulation in Colon Cancer
Integrin Signaling
Regulation Of EMT By Growth Factors Pathway
Threshold

Fig. 2

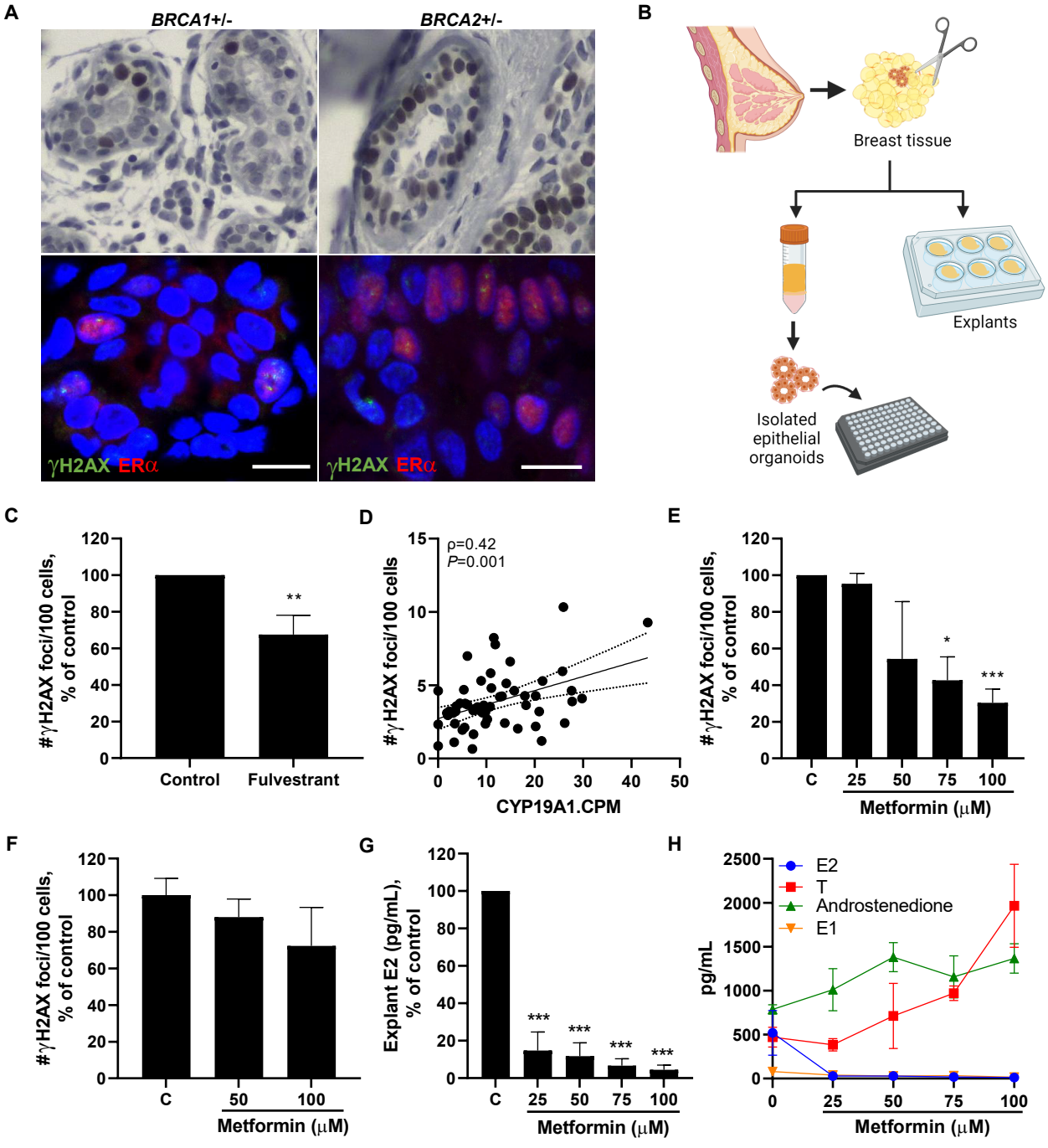
A
BRCA1+/-
BRCA2+/-
γH2AX ERα
γH2AX ERα
B
Breast tissue
Explants
Isolated epithelial organoids
C
#γH2AX foci/100 cells, % of control
**
Control
Fulvestrant
D
ρ=0.42
P=0.001
#γH2AX foci/100 cells
CYP19A1.CPM
E
#γH2AX foci/100 cells, % of control
*
***
C
25
50
75
100
Metformin (μM)
F
#γH2AX foci/100 cells, % of control
C
50
100
Metformin (μM)
G
Explant E2 (pg/mL), % of control
***
***
***
***
C
25
50
75
100
Metformin (μM)
H
E2
T
Androstenedione
E1
pg/mL
0
25
50
75
100
Metformin (μM)

Fig. 3

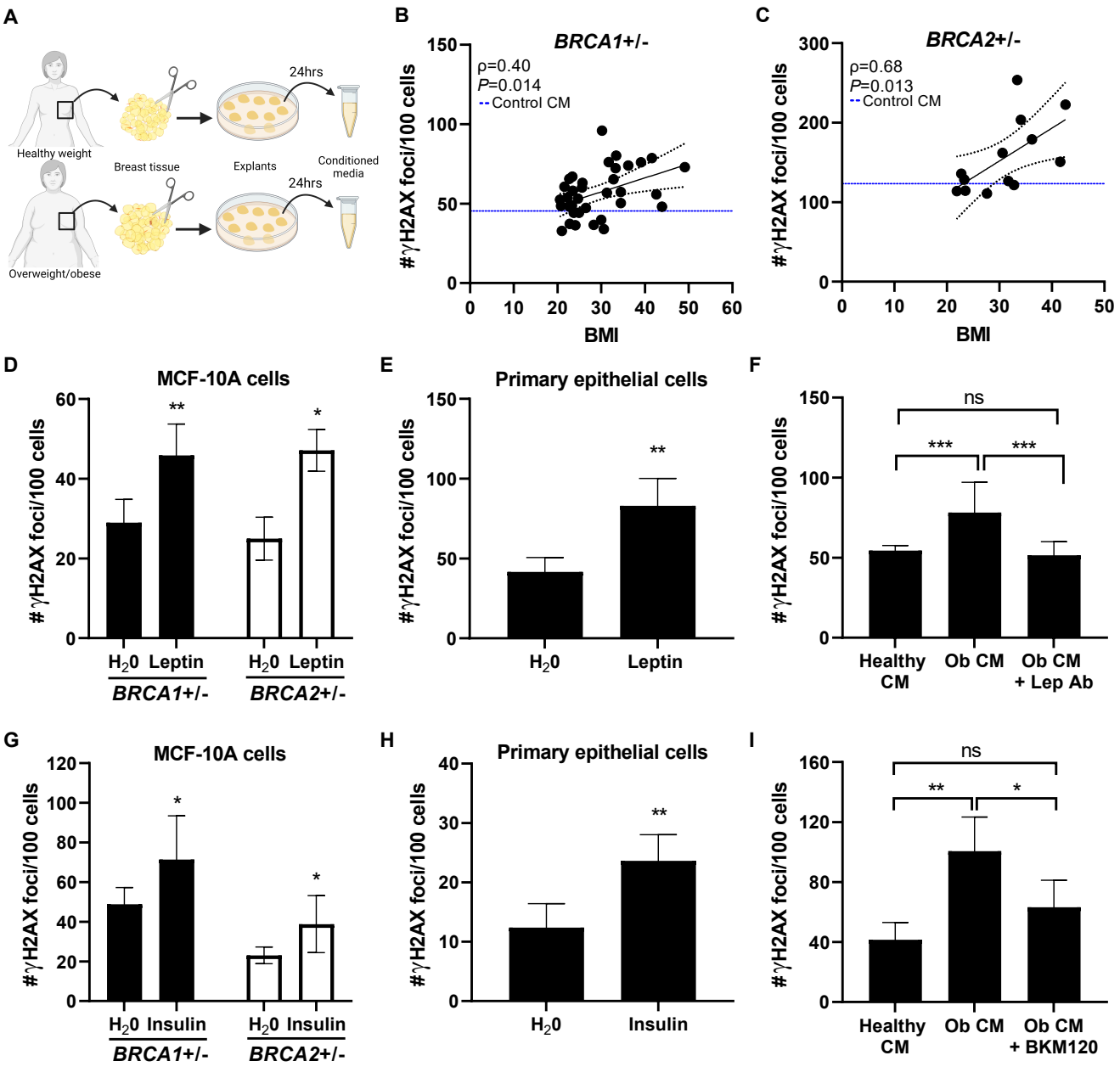
A
Healthy weight
Breast tissue
Explants
24hrs
Conditioned media
Overweight/obese
B
BRCA1+/-
ρ=0.40
P=0.014
Control CM
#γH2AX foci/100 cells
BMI
C
BRCA2+/-
ρ=0.68
P=0.013
Control CM
#γH2AX foci/100 cells
BMI
D
MCF-10A cells
#γH2AX foci/100 cells
H20 Leptin
BRCA1+/-
H20 Leptin
BRCA2+/-
E
Primary epithelial cells
#γH2AX foci/100 cells
H20
Leptin
F
ns
***
***
#γH2AX foci/100 cells
Healthy CM
Ob CM
Ob CM + Lep Ab
G
MCF-10A cells
#γH2AX foci/100 cells
H20 Insulin
BRCA1+/-
H20 Insulin
BRCA2+/-
H
Primary epithelial cells
#γH2AX foci/100 cells
H20
Insulin
I
ns
**
*
#γH2AX foci/100 cells
Healthy CM
Ob CM
Ob CM + BKM120

Fig. 4

A

Top Diseases and Functions	*BRCA1*+/-	WT
Cell viability	-3.154	-2.308
Cell survival	-3.513	-1.828
Proliferation of connective tissue cells	-3.14	-1.753
Chromosomal aberration	2.853	1.846
Organismal death	2.902	1.382
Cell viability of tumor cell lines	-2.355	-1.903
Cell proliferation of tumor cell lines	-2.827	-1.11
Repair of cells	-3.714	N/A
Apoptosis of fibroblast cell lines	-3.358	N/A
Repair of tumor cell lines	-3.338	N/A
Repair of DNA	-3.334	N/A
Productive infection of cervical cancer cell lines	-3.323	N/A
Cell death of connective tissue cells	-1.449	-1.736
Infection by RNA virus	-1.975	1.2
Viral Infection	-2.288	0.826
Proliferation of fibroblast cell lines	-1.566	-1.458
Infection by Retroviridae	-2.999	N/A
Infection by HIV-1	-2.984	N/A
Liver cancer	-2.363	0.6
Malignant genitourinary solid tumor	1.836	1.123
Colon tumor	2.133	0.808
Digestive system cancer	-2.613	-0.313
Tumorigenesis of lymphocytes	0.825	2.078
Infection by lentivirus	-2.861	N/A
Apoptosis of tumor cell lines	0.715	-2.108
Liver tumor	-1.86	0.958
Quantity of cells	-2.318	-0.491
Checkpoint control	-2.756	N/A
Formation of micronuclei	2.756	N/A
Expression of RNA	-0.876	-1.879
Hematologic cancer of cells	1.03	1.717
Breast cancer	1.63	1.109
Gastrointestinal tract cancer	-1.689	-1.026
Hepatobiliary system cancer	-2.426	0.287
Survival of organism	-2.183	0.506
Hematologic cancer	0.345	2.307
Cell death of tumor cell lines	1.17	-1.474
Lymphoma	0.668	1.969
Growth of connective tissue	-2.637	N/A
Neoplasia of leukocytes	0.83	1.801
T-cell malignant neoplasm	1.396	1.214
Multiple cancers	1.198	1.41
Transcription of RNA	-1.116	-1.487
Chromosomal instability	2.603	N/A
Association of chromosome components	-2.596	N/A
Anogenital cancer	1.351	1.242
Hepatobiliary neoplasm	-1.889	0.66
Malignant lymphocytic neoplasm	0.659	1.885
Lymphocytic cancer	0.659	1.885
Neoplasia of blood cells	0.657	1.854

B

DNA damage & repair	*BRCA1*+/-	WT
Chromosomal aberration	2.853	1.846
Repair of cells	-3.714	N/A
Repair of tumor cell lines	-3.338	N/A
Repair of DNA	-3.334	N/A
Checkpoint control	-2.756	N/A
Formation of micronuclei	2.756	N/A
Chromosomal instability	2.603	N/A
Association of chromosome components	-2.596	N/A
Breakage of chromosomes	2.488	N/A
Senescence of cells	1.736	-0.508
Double-stranded DNA break repair of tumor cell lines	-2.241	N/A
Mitosis of tumor cell lines	0.87	1.342
Interaction of DNA	-2.157	N/A
Cell cycle progression	-0.921	-1.202
Metabolism of DNA	-2.09	N/A
Spindle checkpoint of cells	-2.035	N/A
Spindle checkpoint	-2.035	N/A
Chromosomal congression of chromosomes	-2	N/A
DNA replication	-1.909	N/A
Homologous recombination of DNA	-0.485	-1.413
Exchange of sister chromatids	1.641	-0.256
M phase of tumor cell lines	-1.664	N/A
Cycling of centrosome	-1.56	N/A
Spindle checkpoint of tumor cell lines	-1.309	N/A
M phase	-1.232	N/A
Interphase of connective tissue cells	-1.195	N/A
Interphase of fibroblasts	-1.195	N/A
Ploidy of epithelial cells	1.195	N/A
Segregation of chromosomes	-1.062	N/A
M phase of cervical cancer cell lines	-1	N/A
DNA recombination	-0.154	-0.802
Recombination	-0.139	-0.802
Initial DNA end resection	-0.927	N/A
S phase	-0.916	N/A
Spindle checkpoint of cervical cancer cell lines	-0.896	N/A
Re-entry into cell cycle progression	0.878	N/A
Mitosis of cervical cancer cell lines	0.816	N/A
Ploidy	0.811	N/A
Homologous recombination	-0.599	N/A
Interphase	-0.567	N/A
Colony formation	-0.504	N/A
Ploidy of cells	0.501	N/A
Colony formation of cells	-0.464	N/A
DNA damage response of cells	-0.463	N/A
Mitosis	-0.084	-0.355
Shortening of telomeres	0.431	N/A
Duplication of centrosome	-0.426	N/A
Formation of centrosome	-0.426	N/A
Aberration of chromosomes	0.221	N/A
Arrest in G2 phase	N/A	N/A

Positive z-score **Negative z-score**

Fig. 5

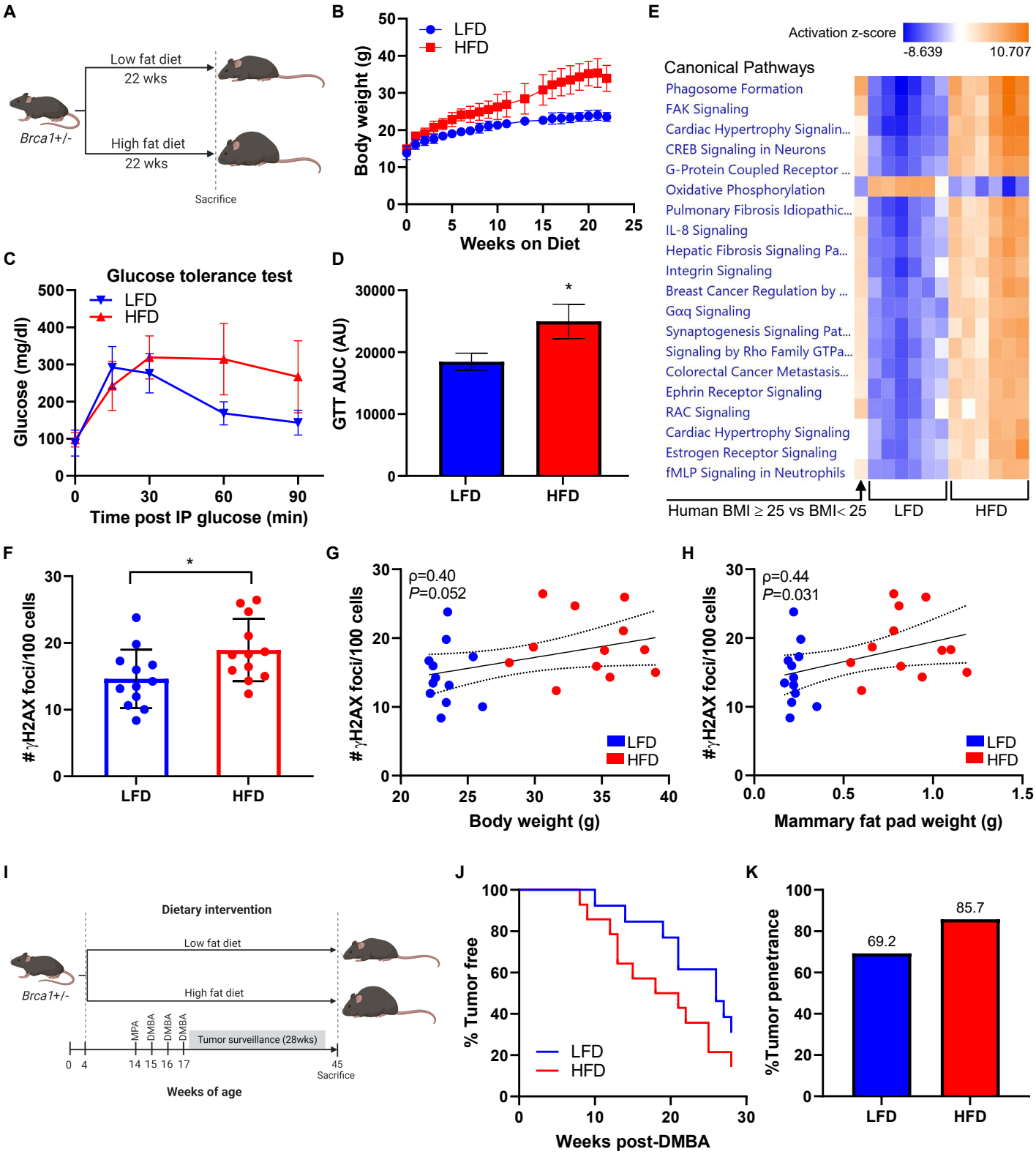
A
Low fat diet
22 wks
Brca1+/-
High fat diet
22 wks
Sacrifice
B
LFD
HFD
Body weight (g)
Weeks on Diet
C
Glucose tolerance test
LFD
HFD
Glucose (mg/dl)
Time post IP glucose (min)
D
GTT AUC (AU)
LFD
HFD
E
Activation z-score
-8.639
10.707
Canonical Pathways
Phagosome Formation
FAK Signaling
Cardiac Hypertrophy Signalin...
CREB Signaling in Neurons
G-Protein Coupled Receptor ...
Oxidative Phosphorylation
Pulmonary Fibrosis Idiopathic...
IL-8 Signaling
Hepatic Fibrosis Signaling Pa...
Integrin Signaling
Breast Cancer Regulation by ...
Gαq Signaling
Synaptogenesis Signaling Pat...
Signaling by Rho Family GTPa...
Colorectal Cancer Metastasis...
Ephrin Receptor Signaling
RAC Signaling
Cardiac Hypertrophy Signaling
Estrogen Receptor Signaling
fMLP Signaling in Neutrophils
Human BMI ≥ 25 vs BMI< 25
LFD
HFD
F
γH2AX foci/100 cells
LFD
HFD
G
ρ=0.40
P=0.052
# γH2AX foci/100 cells
Body weight (g)
LFD
HFD
H
ρ=0.44
P=0.031
# γH2AX foci/100 cells
Mammary fat pad weight (g)
LFD
HFD
I
Dietary intervention
Low fat diet
High fat diet
Brca1+/-
MPA
DMBA
DMBA
DMBA
Tumor surveillance (28wks)
0 4
14 15 16 17
45
Sacrifice
Weeks of age
J
% Tumor free
LFD
HFD
Weeks post-DMBA
K
%Tumor penetrance
69.2
85.7
LFD
HFD

Fig. 6

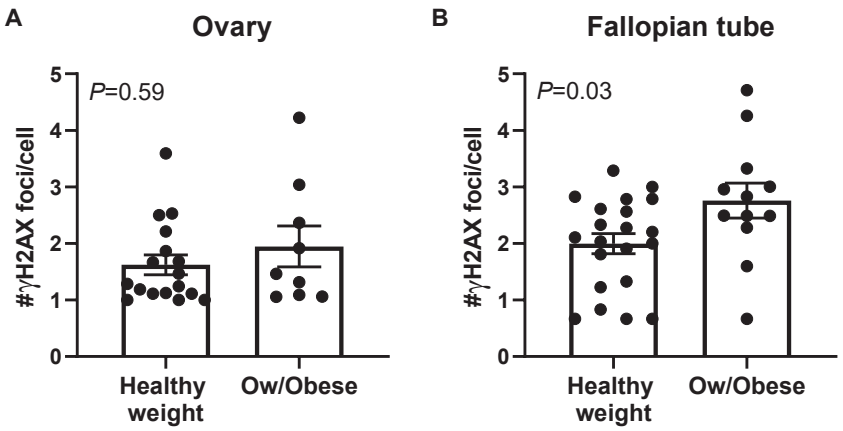
A
Ovary
P=0.59
#γH2AX foci/cell
0
1
2
3
4
5
Healthy weight
Ow/Obese
B
Fallopian tube
P=0.03
#γH2AX foci/cell
0
1
2
3
4
5
Healthy weight
Ow/Obese

Fig. 7

Supplementary Materials

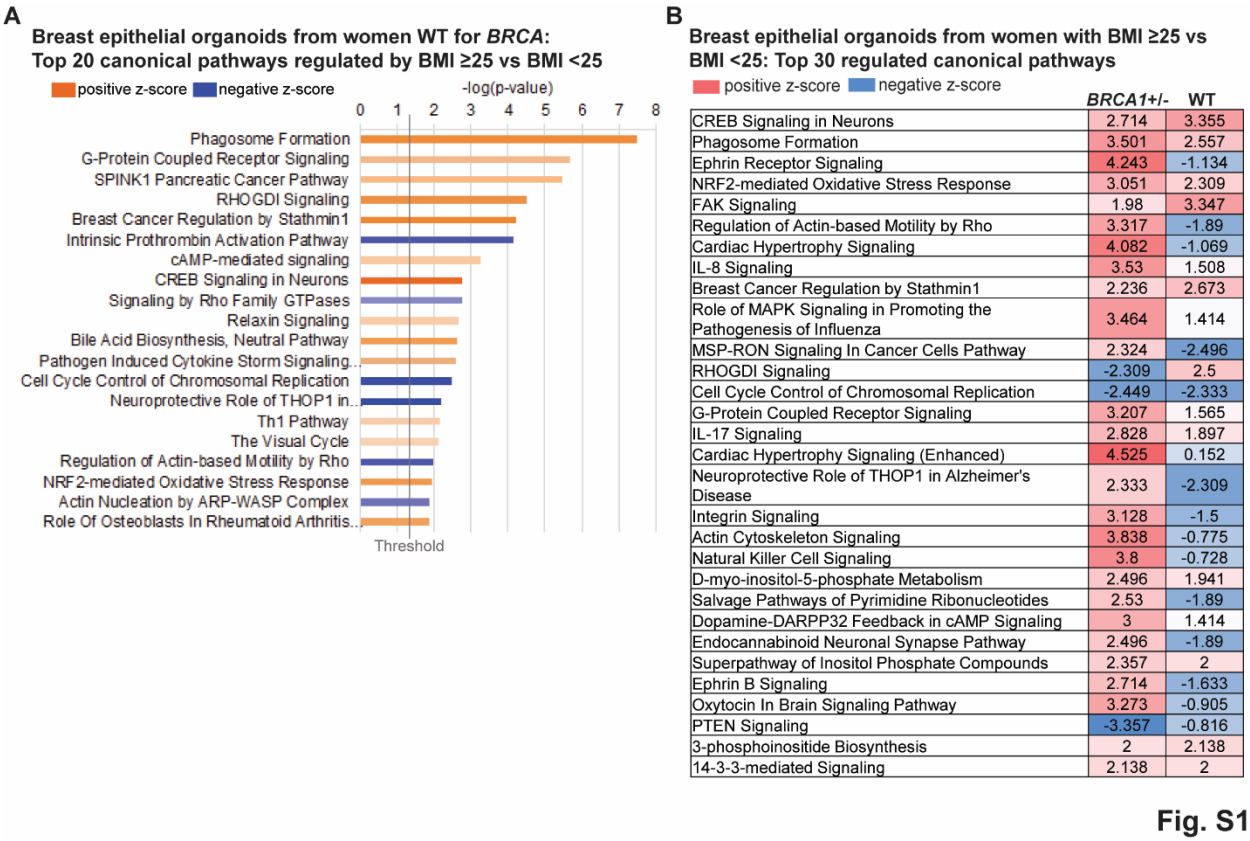

	BRCA1+/-	WT
CREB Signaling in Neurons	2.714	3.355
Phagosome Formation	3.501	2.557
Ephrin Receptor Signaling	4.243	-1.134
NRF2-mediated Oxidative Stress Response	3.051	2.309
FAK Signaling	1.98	3.347
Regulation of Actin-based Motility by Rho	3.317	-1.89
Cardiac Hypertrophy Signaling	4.082	-1.069
IL-8 Signaling	3.53	1.508
Breast Cancer Regulation by Stathmin1	2.236	2.673
Role of MAPK Signaling in Promoting the Pathogenesis of Influenza	3.464	1.414
MSP-RON Signaling In Cancer Cells Pathway	2.324	-2.496
RHOGDI Signaling	-2.309	2.5
Cell Cycle Control of Chromosomal Replication	-2.449	-2.333
G-Protein Coupled Receptor Signaling	3.207	1.565
IL-17 Signaling	2.828	1.897
Cardiac Hypertrophy Signaling (Enhanced)	4.525	0.152
Neuroprotective Role of THOP1 in Alzheimer's Disease	2.333	-2.309
Integrin Signaling	3.128	-1.5
Actin Cytoskeleton Signaling	3.838	-0.775
Natural Killer Cell Signaling	3.8	-0.728
D-myo-inositol-5-phosphate Metabolism	2.496	1.941
Salvage Pathways of Pyrimidine Ribonucleotides	2.53	-1.89
Dopamine-DARPP32 Feedback in cAMP Signaling	3	1.414
Endocannabinoid Neuronal Synapse Pathway	2.496	-1.89
Superpathway of Inositol Phosphate Compounds	2.357	2
Ephrin B Signaling	2.714	-1.633
Oxytocin In Brain Signaling Pathway	3.273	-0.905
PTEN Signaling	-3.357	-0.816
3-phosphoinositide Biosynthesis	2	2.138
14-3-3-mediated Signaling	2.138	2

Fig. S1

Fig. S1. Elevated BMI is associated with distinct changes in gene expression in breast epithelial cells isolated from women who are WT for *BRCA* compared with breast epithelial cells from *BRCA* mutation carriers

(A) IPA analysis of RNA-seq gene expression data showing activation of the top 20 canonical pathways regulated in primary breast epithelial organoids from women WT for *BRCA* with BMI ≥ 25 (n=8) relative to women with BMI < 25 (n=11) with an absolute value z-score of > 1. The length of the bars are determined by the Fisher's Exact Test *P* value with entities that have a -log(p-value) > 1.3 shown. (**B**) Top 30 canonical pathways regulated in breast epithelial organoids from women with BMI ≥ 25 relative to BMI < 25, comparing activation z-scores in *BRCA*+/- mutation carriers with non-carriers. Activation z-scores are color coded with gradations of red

representing a positive z-score and gradations blue representing a negative z-score. Significantly regulated pathways as defined by -log(p-value) >1.3 are shown.

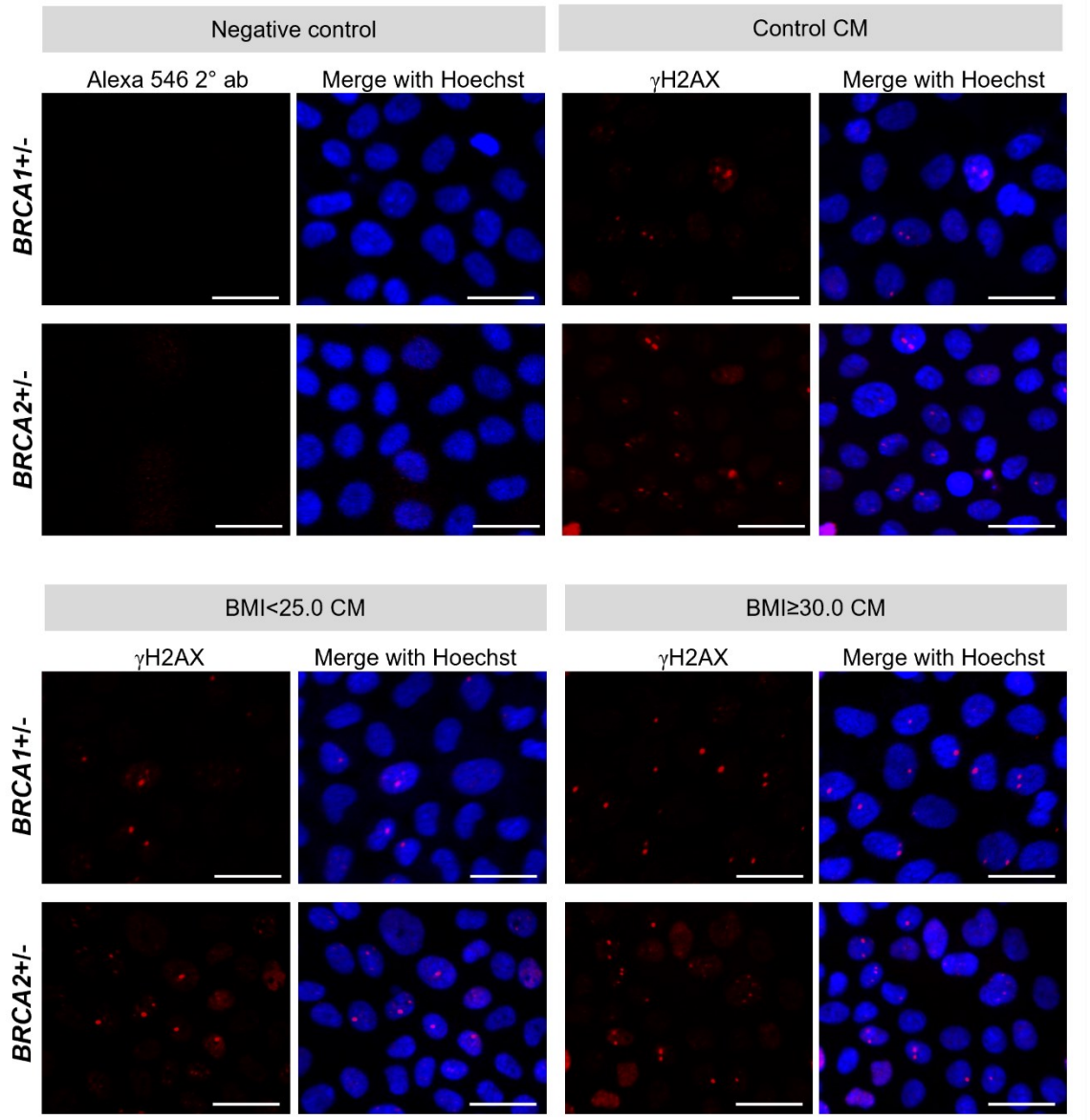

Fig. S2

Fig. S2. Representative confocal images of γH2AX foci immunofluorescence staining in *BRCA1*+/- and *BRCA2*+/- MCF-10A cells. Top half shows representative γH2AX foci (red) in control conditions, including negative control (cells incubated with secondary antibody only and no primary antibody) and control CM treatment (cells treated with media used for collection of CM which has not been exposed to conditioning by adipose explants). Foci are shown merged with nuclei stained with Hoechst (blue). Bottom half shows representative γH2AX staining in cells treated with CM derived from women with BMI < 25 or ≥ 30. *BRCA1*+/- and *BRCA2*+/- MCF-10A cells are shown. Scale bar = 30μM.

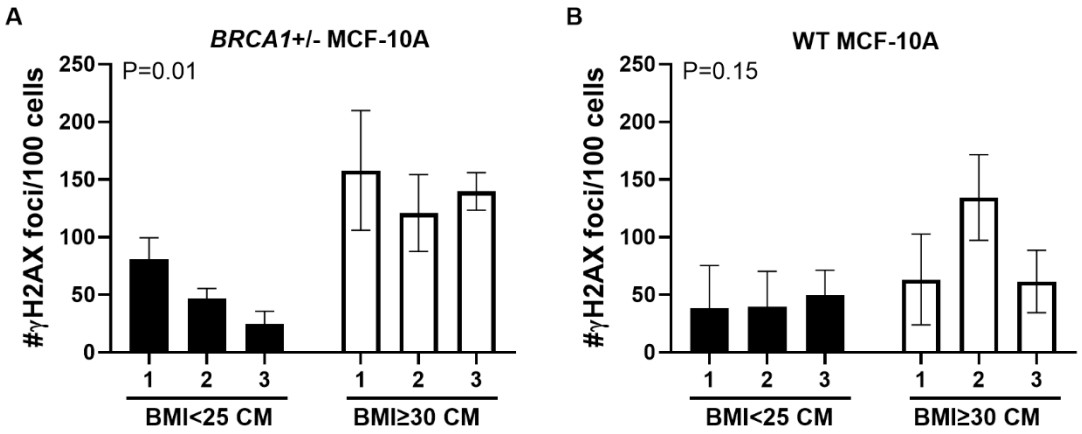

Fig. S3

Fig. S3. Breast adipose conditioned media from women with BMI ≥ 30 stimulates more DNA damage in *BRCA1*+/- MCF-10A cells compared to conditioned media from women with BMI < 25.

(A) *BRCA1*+/- MCF-10A cells and (**B**) WT MCF-10A cells were treated with breast adipose conditioned media (CM) collected from women with BMI< 25 (n=3) or BMI ≥ 30 (n=3). DNA damage was assessed by IF (#γH2AX foci/100 cells) after 24 hours treatment. *P* value represents a comparison of average DNA damage in cells treated with CM from breast tissue from women with BMI < 25 vs BMI ≥ 30 by Student's T test. Data is presented as mean +/- SD.

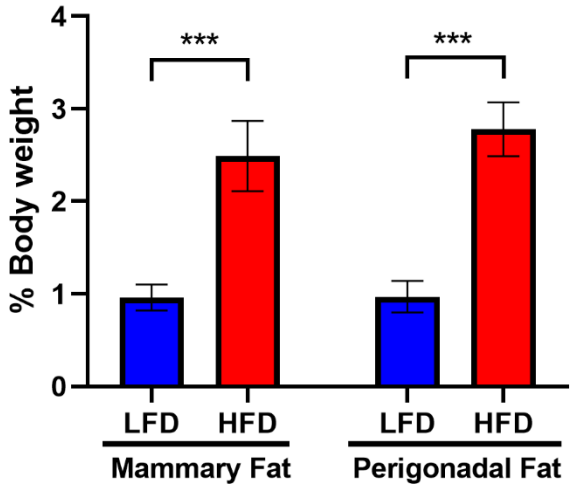

Fig. S4

Fig. S4. *Brca1*+/- mice fed high-fat diet have significantly greater accumulation of body fat compared to *Brca1*+/- mice fed low-fat diet

Wet weight of inguinal mammary fat pads (subcutaneous fat) and perigonadal fat (visceral fat) at the time of euthanasia, expressed as % of whole-body weight in female *Brca1*+/- mice fed low-

fat diet (LFD) or high-fat diet (HFD) for 22 weeks (n=12/gp). Student's T test was used to determine significant differences between LFD and HFD mice. Data is presented as mean +/- SD, ***P<0.001.

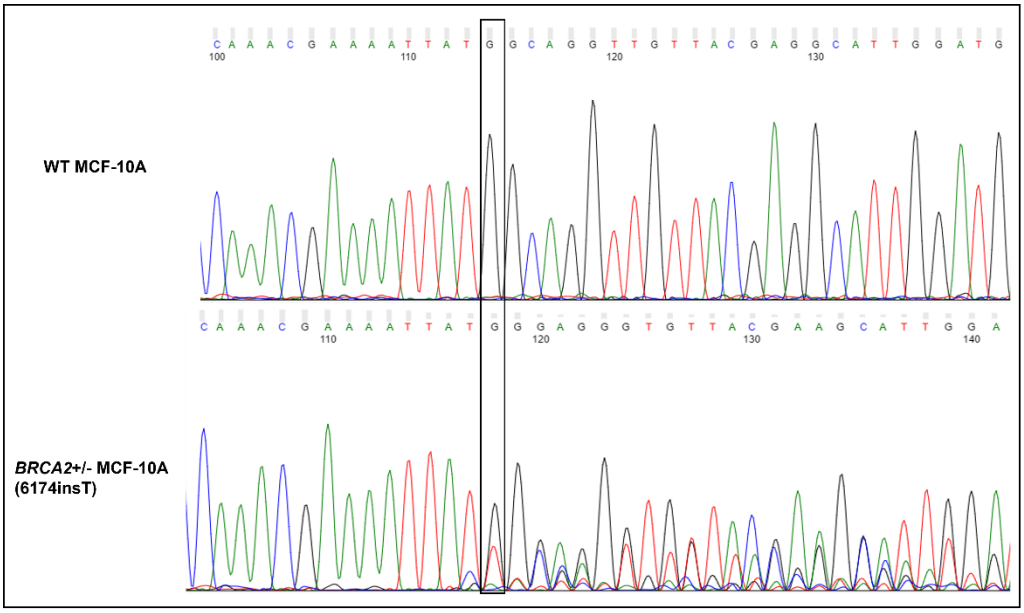

Fig. S5

Fig. S5. Generation of MCF-10A cells carrying a *BRCA*2 heterozygous mutation

CRISPR-Cas9 gene editing was utilized to generate an isogenic MCF-10A cell line carrying a heterozygous *BRCA*2 mutation (6174insT). Candidate clones were submitted for Sanger sequencing (Genewiz) and a clone exhibiting a heterozygous mutation as determined by the sequencing chromatogram shown in the figure was selected for downstream *in vitro* studies.

Table S6. Genes involved in "Repair of DNA" significantly regulated in *BRCA1*+/- MCF-10A cells treated with breast adipose CM derived from women with obesity compared to women with healthy weight

Gene	Log2FC	*P* value
TOP2A	-2.971	0.0216534
EXO1	-2.407	0.0041363
TNF	-2.366	0.0331524
NEIL3	-1.56	0.0454292
BLM	-1.554	0.0240665
RAD54L	-1.55	0.0265702
BRCA2	-1.362	0.0200827
XRCC2	-1.228	0.0213886
BRIP1	-1.196	0.0160386
BRCA1	-1.082	0.016198
FANCA	-0.927	0.0374675
FANCD2	-0.868	0.0456246
TRIP13	-0.813	0.0072051
FANCM	-0.638	0.0156575
ANKRD32	-0.479	0.0115143
MDM2	-0.435	0.0095298
FOS	-0.416	0.0424863
HMGA2	-0.384	0.0298825
RRM2B	-0.383	0.0158232
USP45	-0.372	0.0033442
UCHL5	-0.369	0.0016047
OTUD6B	-0.335	0.0271729
RAD18	-0.334	0.0322693
HMGB1	-0.325	0.0245722
TCEA1	-0.319	0.0165788
DEK	-0.304	0.0111833
PMS1	-0.29	0.0165185
PHF6	-0.271	0.0112097
HNRNPU-AS1	-0.269	0.0298011
RIF1	-0.267	0.0259465
TDG	-0.259	0.0321275
USP15	-0.255	0.0472664
BCLAF1	-0.254	0.0267277
RB1	-0.253	0.0264751
SMCHD1	-0.245	0.0040162
MRE11A	-0.235	0.0092542
FAM175A	-0.224	0.0329318
RAD21	-0.22	0.0433965
CHEK1	-0.211	0.0422347
THOC1	-0.206	0.0421476
WRN	-0.191	0.0306967
EIF3F	0.157	0.0450842

PRKCZ	0.259	0.032568
PIK3C2B	0.29	0.0040939
CBX8	0.338	0.0150821
CEBPA	0.438	0.0047412
CLU	0.613	0.0099281

Tables S1-S5 and S7-S8 can be found in Data File S1 (multi-tab Excel file)

Supplementary Methods

Immunofluorescence and immunohistochemistry staining

Human breast, ovary, and fallopian tube tissue: unstained sections were cut from paraffin blocks of embedded tissue or tissue microarrays. Slides were deparaffinized by immersion in xylene and rehydrated in decreasing concentrations of ethanol. Antigen retrieval was conducted by immersing the slides in citrate buffer (10mM citric acid, 0.05% Tween 20, pH 6.0), heating in a microwave, and cooling for 30 minutes at room temperature. Slides were then washed, blocked for 1 hour with CAS blocking reagent, and incubated with primary γH2AX antibody overnight at 4°C. Slides were then washed and incubated with Alexa Fluor 546 secondary antibody and Hoechst stain for 2 hours. Following this incubation period, all slides were washed and mounted with ProLong Gold until imaging by confocal microscopy.

Mouse mammary gland: Similar protocol as described above was conducted with sections from paraffin embedded mouse mammary gland tissue, however following antigen retrieval, staining procedures were conducted in accordance with the manufacturer's protocol for the M.O.M. immunodetection kit with some modifications. In brief, slides were incubated in M.O.M. Mouse IgG blocking reagent for 1 hour, washed, and incubated with M.O.M. diluent for

5 min followed by incubation with primary γH2AX antibody in M.O.M diluent overnight at 4°C. Slides were washed, incubated with secondary antibody and Hoechst stain in M.O.M diluent for 2 hours, washed and mounted.

Plated breast epithelial cells: Primary breast epithelial cells, *BRCA1* and *BRCA2* heterozygous MCF-10A cells, or WT MCF-10A cells were fixed in ice cold methanol for 15 mins at -20°C, washed and blocked with CAS block reagent for 1 hour followed by overnight incubation with primary γH2AX antibody at 4°C. The next day cells were washed, incubated with secondary antibody and Hoechst for 2 hours and imaged by confocal microscopy.

ERα IHC and IF colocalization of ERα & γH2AX: IHC was conducted on breast tissue sections from *BRCA1* and *BRCA2* mutation carriers to detect presence of ERα positive epithelial cells. Slides were deparaffinized in xylene and re-hydrated followed by 1 hour antigen retrieval (citrate buffer 0.01 M, pH 6.0) at 95°C and 30 minutes cooling at room temperature. Slides were rinsed and then incubated for 5 minutes with 3% H_20_2 to inhibit endogenous peroxidase activity. Vectastain ABC-HRP (Peroxidase, Anti-Mouse IgG) immunodetection kit (Vector Labs #PK-4002) was then used following the manufacturer's protocol. In brief, after 30-minute incubation in blocking serum, primary ERα antibody (Leica Biosystems #ER-6F11-L-F, 1:50 dilution) was added for 1 hour at room temperature followed by biotinylated secondary antibody incubation for 30 minutes. Slides were washed, developed with DAB substrate kit (Vector Labs #SK-4100) and counterstained with hematoxylin for visualization of ERα positive epithelial cells. In γH2AX co-localization studies by IF, a similar protocol through antigen retrieval was followed as described above. Slides were then blocked for 1 hour with CAS block and incubated with primary ERα and γH2AX (NB100-384, 1:300) antibodies overnight at 4°C. Slides were washed

and incubated with anti-Mouse Alexa Fluor 546 and anti-Rabbit Alexa Fluor 488 secondary antibodies with Hoechst.

RNA-seq studies & computational analysis:

Total RNA was extracted from samples in all studies by Trizol lysis and RNeasy Mini Kit (Qiagen) following the manufacturer's protocols. Samples were submitted for RNA-seq at the Genomics Resources Core Facility (GRCF, Weill Cornell Medicine). Additional details for each study are described below:

Human breast tissue: To assess differences in breast tissue gene expression in *BRCA* mutation carriers with BMI ≥ 25 (n=64) vs relative to carriers with BMI < 25 (n=67), snap frozen non-tumorous breast tissue was obtained from women who had previously undergone prophylactic or therapeutic mastectomy surgery at MSKCC. In the therapeutic mastectomy cases, only normal breast tissue from quadrant free of tumor or contralateral breast, as determined by a pathologist, was collected and snap frozen. Sequencing libraries were constructed at the GRCF following the Illumina TrueSeq Stranded Total RNA library preparation protocol with ribosomal RNA depletion. The libraries were sequenced with paired-end 51 bp on the Illumina HiSeq4000 sequencing platform. Raw sequenced reads were pseudoaligned to the human reference genome (UCSC hg19) using the RNA-seq quantification program Kallisto as previously described (*69*) and transcript abundance was quantified to obtain and raw counts. Normalization of the RNA-seq raw read counts and pairwise statistical analysis were performed using the DESeq2 package (version 1.30.1)(*70*). Differentially expressed genes (DEG) were determined by comparing cases with BMI ≥ 25 relative to cases with BMI < 25 or

DNA damage Q4 relative to Q1. The tissue RNA-seq heatmap plot (**Fig. 2A**) was generated with R pheatmap package, using the DESeq2 normalized CPM values.

DEGs with Log2FC of >0.3 and <-0.3 and *P* value<0.05 were uploaded to Ingenuity Pathway Analysis (IPA, Qiagen) for data visualization and analysis. The estrogen metabolism heatmap (**Fig. 2C**) was generated by standardizing values relative to data across cases for each gene returning a normalized value from a distribution characterized by the mean and standard deviation of each gene.

Breast epithelial organoids: To assess differences in breast epithelial cell gene expression in *BRCA* mutation carriers with BMI ≥ 25 (n=9) relative to carriers with BMI < 25 (n=10) and in women WT for *BRCA* with BMI ≥ 25 (n=8) relative to women with BMI < 25, breast epithelial organoids were isolated from patients as described in the main text **Materials & Methods** section. Sequencing libraries were constructed at the GRCF following the Illumina TruSeq Stranded mRNA library preparation protocol (Poly-A selection and Stranded RNA-Seq). The libraries were sequenced with paired-end 50 bp on the Illumina HiSeq4000 sequencing platform. All reads were independently aligned with STAR_2.4.0f1 (*71*) for sequence alignment against the human genome sequence build hg19, downloaded via the UCSC genome browser and SAMTOOLS v0.1.19 (*72*) for sorting and indexing reads. Normalization of the RNA-seq raw read counts, and pairwise statistical analysis were performed as described above. DEGs were determined by comparing the cases with BMI ≥ 25 relative to cases with BMI <25. All DEGs with *P* value <0.05 were uploaded to IPA for data visualization and analysis.

MCF-10A cells: To assess gene expression changes associated with treatment with obese breast adipose CM, MCF-10A cells carrying a heterozygous *BRCA1* mutation or WT for *BRCA1* were treated with breast adipose CM derived from women with BMI ≥ 25 or BMI < 25 (n=3/gp).

RNA was extracted after 24-hour treatment for RNA-seq. Sequencing libraries were constructed at the GRCF following the Illumina TruSeq Stranded mRNA library preparation protocol (Poly-A selection and Stranded RNA-Seq). The libraries were sequenced with paired-end 50 bp on the Illumina HiSeq4000 sequencing platform. All reads were independently aligned with STAR_2.4.0f1 (*71*) for sequence alignment against the human genome sequence build hg19, downloaded via the UCSC genome browser and SAMTOOLS v0.1.19 (*72*) for sorting and indexing reads. Cufflinks (2.0.2) (*73*) was used to estimate the expression values (FPKMS), and GENCODE v19 (*74*) GTF file for annotation. The gene counts from htseq-count and DESeq2 Bioconductor package (*70*) were used to identify DEGs. All DEGs with *P* value <0.05 were uploaded to IPA for data visualization and analysis.

Mouse mammary fat pads: To assess differences in mammary fat pad gene expression in association with obesity, mammary fat pads were harvested from female *Brca1*+/- mice fed high-fat diet-fed or low-fat diet-fed (n=6/gp) followed by RNA extraction for RNA-seq. Sequencing libraries were constructed at the GRCF following the Illumina TruSeq Stranded mRNA library preparation protocol (Poly-A selection and Stranded RNA-Seq). The libraries were sequenced with paired-end 50 bp on the Illumina NovaSeq 6000 sequencing platform. The raw sequencing reads in were processed through bcl2fastq 2.19 (Illumina) for FASTQ conversion and demultiplexing. After trimming the adaptors with cutadapt (version1.18), RNA reads were aligned and mapped to the GRCm38 mouse reference genome by STAR (Version2.5.2) (*71*), and transcriptome reconstruction was performed by Cufflinks (Version 2.1.1). The abundance of transcripts was measured with Cufflinks in Fragments Per Kilobase of exon model per Million mapped reads (FPKM). Normalization of the RNA-seq raw read counts and pairwise statistical

analysis were performed using the DESeq2 package (version 1.30.1) (*70*). DEGs were determined by comparing the high-fat diet group relative to the low-fat diet group.

Heatmaps showing comparisons between RNA-seq data from mouse and human mammary tissue were generated using IPA. Briefly, mouse raw read counts were standardized relative to data across all mouse samples for each gene returning a normalized value from a distribution characterized by the mean and standard deviation of each gene. Top canonical pathways affected based on DEGs from human cases with BMI ≥ 25 relative to cases with BMI < 25 were then compared to standardized values from mouse samples.

Generation of *Brca1*+/- mice

We generated global *Brca1* heterozygous mice (*Brca1*+/-) by crossing $Brca1^{flox\ 5\text{-}13/flox\ 5\text{-}13}$ (*75, 76*) with CMV-Cre mice (JAX strain #006054, (*77*)) to produce global $Brca1^{D5\text{-}13/+}$ mice. Genotyping was performed via PCR with primers as previously described (*75*). No offspring were found to be homozygous knockout for *Brca1* suggesting that complete loss of *Brca1* is embryonically lethal. These mice were backcrossed to a C57Bl/6 strain over 20 times. Genetic testing of mice following backcrossing was performed at Charles River Genetic Testing Services and demonstrated 98.6% fidelity with C57Bl/6 inbred strains.

Generation of *BRCA2* heterozygous MCF-10A cell line

We used CRISPR-Cas9 gene editing to generate an isogenic MCF-10A cell line carrying a clinically-relevant heterozygous *BRCA2* mutation (6174insT). The forward (A) and reverse (B) sgRNA cloning primers were as follows:

A: CACCGGCCAAACGAAAATTATGGC

B: AAACGCCATAATTTTCGTTTGGCC

These primers were annealed and cloned following standard procedures using the BsmBI/EcoRI site of the *pLenti-U6-sgRNA-tdTomato-P2A-Blas* (LRT2B) vector. WT MCF-10A cells stably expressing an optimized *pLenti-Cas9-P2A-Puro* lentiviral vector were transduced with sgRNAs and underwent Blasticidin selection followed by isolation of single clones using the limiting dilution assays, as described previously (*78, 79*). Candidate colonies expressing TdTomato were submitted for Sanger sequencing (Genewiz) to identify clones exhibiting a heterozygous *BRCA2* mutation (**Fig. S5**). Analysis of sequencing data showed insertion of a thymine (T) nucleotide 5670bp from the start of the open reading frame (ATG) that led to an early stop codon at amino acid 1889. This mutation was maintained upon re-sequencing after multiple passages. The clonal population was expanded and utilized for downstream *in vitro* studies.

Quantitative steroid analysis in breast explants

Snap frozen breast tissue explants were lyophilized and homogenized and 10 mg of individual samples were used in each assay. After spiking with 20 µL of an internal standard mixture (2,2,4,6,6,21,21,21-d_8-17α-hydroxyprogesterone, 1 µg/mL; 2,2,3,4,4,6-d_6-dehydroepiandrosterone and 2,2,4,6,6,17α,21,21,21-d_9-progesterone, 0.5 µg/mL; 16,16,17-d_3-testosterone and 9,11,12,12-d_4-cortisol, 0.25 µg/mL; 2,4,16,16-d_4-17β-estradiol, 0.2 µg/mL) and

mixed with 1 mL of 0.2 M phosphate buffer (pH 7.2), the sample was pulverized using a TissueLyser (Qiagen, Hilden, Germany) at 25 Hz for 10 min with three zirconia beads (3.0 mm I.D., Toray Industries, Tokyo, Japan) and centrifuged at 12,000 rpm for 10 min twice. The combined supernatant was loaded onto a preconditioned solid-phase extraction (SPE) cartridge (Oasis HLB; 3 mL, 60 mg; Wasters, Milford, MA, USA), the SPE cartridge was washed with 1 mL of water twice and eluted with 2 mL of methanol and 2 mL of 90% methanol. The combined eluate was evaporated under a nitrogen stream at 40°C. The sample was dissolved in 1 mL of 0.2 M acetate buffer (pH 5.2) and 100 μL of 0.2% ascorbic acid solution. It was then extracted with 2.5 mL of methyl *tert*-butyl ether twice. The organic solvent was evaporated under a nitrogen stream and further dried in a vacuum desiccator with P_2O_5/KOH for at least 30 min. Finally, the dried residue was derivatized with 50 μL of *N*-methyl-*N*-trifluorotrimethylsilylacetamide/ammonium iodide/dithioerythritol (500:4:2, v/w/w) at 60°C for 20 min. Then 2 μL of the final mixture was injected into the GC-MS system.

In samples with no quantifiable estrogens, the estrogen assay with improved analytical detectability (*80*) was performed from an additional 10 mg of homogenized breast tissues. For the calibration sets, steroid-free breast tissue was freshly prepared 1 day before the experiment. Human breast samples (50 mg) were pulverized in 1 mL methanol/chloroform (1:1, v/v) with 4 zirconia beads at 25 Hz for 5 min followed by centrifugation twice at 12,000 rpm for 3 min, and then supernatants were discarded. The remaining tissue sample was washed with l mL of chloroform/0.6 M methanolic HCl (1:1, v/v), sonicated for 5 min, and centrifuged at 12,000 rpm for 3 min three times. All supernatants were also discarded. To eliminate residual methanolic HCl, 1 mL of 20% ethanol was added for washing five times. Tissue samples were then frozen at -80 °C until used. No steroid was detectable in GC-MS chromatogram.